Fermi National Accelerator Laboratory

FERMILAB–PUB–88/168-T
November 1988

The Complete Computation of High-p_T W and Z Production in 2nd-Order QCD

PETER B. ARNOLD

High Energy Physics Division
Argonne National Laboratory, Argonne, IL 60439

and

Fermi National Accelerator Laboratory, P.O. Box 500, Batavia, IL 60510

M. HALL RENO

Departmento de Física
Centro de Investigacion y de Estudios Avanzados del I.P.N.
Apartado Postal 14-740, Mexico 07000, D.F.

and

Fermi National Accelerator Laboratory, P.O. Box 500, Batavia, IL 60510

ABSTRACT

We present a full computation of $d\sigma/dq_T^2$ for W, Z and virtual γ production to second-order in QCD. This includes qg, gg, and singlet $q\bar{q}+qq$ collisions in addition to the usual non-singlet $q\bar{q}+qq$. The primary motivation is the importance of quark-gluon collisions at Tevatron energies. Attention is restricted to high and moderate q_T, avoiding the resummation necessary at small transverse momentum. We give analytic results for all constituent cross-sections $d\sigma/dq_T^2dy$ and, for W and Z production, numerically convolute them with structure functions.

Operated by Universities Research Association Inc. under contract with the United States Department of Energy

1. Introduction

The transverse momentum (q_T) distribution of single W production provides a useful test of the standard model and a means of measuring α_s.[1] Furthermore, W production is a background to new physics. In this paper, we examine the q_T distributions of virtual photons and weak gauge bosons. We restrict our attention to large q_T and calculate to second order in QCD. By including the full α_s^2 contribution, we reduce the theoretical errors associated with the leading order ($O(\alpha_s)$) result. Using these expressions together with parton distribution functions evolved at two-loop order, we make predictions for the q_T distributions at the SPS and Tevatron Colliders.

The second-order corrections have previously been calculated for the most significant processes at CERN energies: the non-singlet contribution to $q\bar{q}$ annihilation.[2,3] At Tevatron energies, however, quark-gluon scattering is equally important.⋆ This process has already been approached for the specific case of $qg \rightarrow W + 2\,\text{jets}$.[4] The technique is to calculate the amplitude and then perform all of the phase-space integrals numerically. Unfortunately, such computations are valid only when the jets are well separated; singularities appear when the jets become collinear with each other or the beam axis. These singularities are related to the break-down of perturbation theory for the differential cross-section in those cases. For example, when the invariant mass s_2 of the two jets becomes small, powers of α_s are countered by factors of large logarithms, $\ln s_2$, of the small scale. For small, fixed s_2, the differential cross-section cannot then be calculated perturbatively. If we were really interested in the cross-section as a function of s_2, we would have to perform some sort of resummation to proceed.

The details of the small s_2 behavior are not necessary if we are interested in the inclusive cross-section for producing a W with any number of jets. Integrating over the phase space of the jets, no small scale remains to give large logarithms

⋆ For definiteness, we discuss W production. We loosely use the terms "final state parton" and "jet" interchangably.

and so high-order contributions should be controlled. For 2-jet production, this phase space integral diverges as the jets become collinear. The divergence is cancelled by a similar divergence in the one-loop corrections to single-jet production. One can cancel the divergences only after integrating over the relative phase-space of the two jets. The complexity of the calculation lies in that this integral must therefore be performed analytically rather than numerically.

When the W has small transverse momentum q_T, there is again a small scale and large logarithms $\ln(q_T/Q^2)$. Perturbation theory for $d\sigma/dq_T^2$ breaks down and one must either perform a resummation or restrict attention to the total cross-section σ by integrating analytically in q_T. These techniques have been carried out to first order in QCD[5], and some of the second-order terms have been analyzed in the $q_T \to 0$ limit.[6] We have attempted neither method with our second-order results and so do not consider very small values of q_T.

Our purpose in this paper will be to extend the previous work on non-singlet $q\bar{q} + qq$ scattering to qg, gg, and singlet $q\bar{q} + qq$ scattering. This will encompass all of the second-order processes. We do not distinguish the polarizations of the W bosons.

The first-order diagrams L for W production through $q\bar{q}$ annihilation are shown in Fig. 1.† Part of the second-order contribution comes from the interference of these diagrams with the one-loop corrections V of Fig. 2. The rest comes from two-jet production accompanying the W as in the diagrams G of Fig. 3. The diagrams for W production through qg scattering can be obtained from L, V, and G by crossing. Those for production through gg scattering can be similarly obtained from G alone. The diagrams F of Fig. 4 give the remaining contributions to $q\bar{q}$ scattering. The diagrams H of Fig 5 are for qq scattering. H_5 through H_8 should be included only if either the initial two quarks or final two quarks are identical.

† The diagrams of Figs. 1 to 5 are taken from Ref. [2].

After notational preliminaries in Section 2, we outline the calculational procedure using dimensional regularization in Section 3. A discussion of how to convert from $\overline{\mathrm{MS}}$ factorization to any other scheme is described in Section 4. In Section 5, we demonstrate that we can sideskip most of the difficulties associated with γ_5 in dimensional regularization. Finally, in Section 6, we discuss numerical techniques and results for W and Z production at the SPS and Tevatron Colliders. The analytic parton level cross-sections for γ^* production with $\overline{\mathrm{MS}}$ factorization appear in Appendix A. Recipes for converting these formulae to W or Z production are shown in Appendix B.

2. Notation

The four-momenta of the colliding hadrons are P_1 and P_2 while those of the colliding partons are p_1 and p_2. q is the four-momenta of the produced W boson, Z boson, or virtual photon; $\vec{q}_T$ and y are its transverse momentum and rapidity; and $Q^2 \equiv q^2$. The hadronic and constituent Mandelstam variables are defined by:

$$S = (P_1 + P_2)^2, \quad T = (P_1 - q)^2, \quad U = (P_2 - q)^2; \tag{2.1}$$

$$s = (p_1 + p_2)^2, \quad t = (p_1 - q)^2, \quad u = (p_2 - q)^2. \tag{2.2}$$

When two-jets accompany the W, their invariant mass s_2 is given by

$$s_2 = s + t + u - Q^2. \tag{2.3}$$

s_2 sometimes appears in distributions as $1/(s_2)_{A+}$ or $(\ln(s_2)/s_2))_{A+}$ which are defined by

$$\int_0^A \mathrm{d}s_2\, \frac{1}{(s_2)_{A+}} f(s_2) = \int_0^A \mathrm{d}s_2\, \frac{1}{s_2}\big(f(s_2) - f(0)\big), \tag{2.4}$$

$$\int_0^A \mathrm{d}s_2\, \left(\frac{\ln s_2}{s_2}\right)_{A+} f(s_2) = \int_0^A \mathrm{d}s_2\, \frac{\ln s_2}{s_2}\big(f(s_2) - f(0)\big). \tag{2.5}$$

A is generally used for the upper limit of s_2 integrations and appears explicitly in some formulas.

The group structure of QCD is handled generically with $N_{\rm C}$ the dimension of a single fermion representation and the Casimir $C_{\rm F}$ defined by $\sum {\rm T}^a{\rm T}^a = C_{\rm F}$. For QCD, these are

$$N_{\rm C} = 3, \qquad C_{\rm F} = \frac{4}{3}. \tag{2.6}$$

$T_{\rm R}$ is half of the number of fermion flavors and so for five flavors is

$$T_{\rm R} = \frac{5}{2}. \tag{2.7}$$

3. Procedure

We will now briefly review the procedure of the calculation to fix notation and indicate to the reader what is involved. Much of this discussion is taken from Ellis *et. al.*, and we refer the reader there or to several reviews for more detail.[2,7]

We want to calculate a quantity $d\tilde{\sigma}$ that can be convoluted with structure functions to obtain the hadronic cross-section:

$$\frac{d\sigma_{AB}}{dq_T^2\, dy} = \sum_{i,j} \int dx_1\, dx_2\; f_i^A(x_1, M^2)\; f_j^B(x_2, M^2)\; \frac{s d\tilde{\sigma}_{ij}}{dt\, du}(\alpha_s(M^2), x_1 P_1, x_2 P_2). \tag{3.1}$$

A and B indicate hadron flavors; i and j indicate parton flavors. There are two sources of terms subleading in α_s: those from subleading terms of $d\tilde{\sigma}$ and those from subleading terms in the definition and evolution of the structure functions. Both will appear in the bare calculation of parton cross-sections and must be disentangled to yield $d\tilde{\sigma}$.

STEP 1. Calculate the bare result $s d\sigma/dt du$ of the Feynman graphs. The loop integrals and the phase space integrals for the particles accompanying the W are done with dimensional regularization. We will denote the first and second-order contributions by $d\sigma^{(1)}$ and $d\sigma^{(2)}$.

STEP 2. Fix your conventions for defining the relationship between the renormalized and bare structure functions:

$$f_i^A(x,M^2) = \int_x^1 \frac{\mathrm{d}z}{z} \left[\delta_{ij}\delta(z-1) + \frac{\alpha_s}{2\pi} R_{i\leftarrow j}(z,M^2)\right] \; f^A_{j,\mathrm{bare}}\left(\frac{x}{z}\right). \tag{3.2}$$

In general, R has the form,

$$R_{i\leftarrow j}(z,M^2) = -\frac{1}{\epsilon} P_{i\leftarrow j}(z) \frac{\Gamma(1-\epsilon)}{\Gamma(1-2\epsilon)} \left(\frac{4\pi\mu^2}{M^2}\right)^{\epsilon} \; + \; C_{i\leftarrow j}(z), \tag{3.3}$$

where the $O(\epsilon)$ pieces are irrelevant and where the P are the Altarelli-Parisi functions:

$$\begin{aligned}
P_{q\leftarrow q}(z) &= C_\mathrm{F}\left[\frac{1+z^2}{(1-z)_+} + \frac{3}{2}\delta(z-1)\right], \\
P_{g\leftarrow q}(z) &= C_\mathrm{F}\frac{1+(1-z)^2}{z}, \\
P_{g\leftarrow g}(z) &= 2N_\mathrm{C}\left[\frac{1}{(1-z)_+} + \frac{1}{z} + z(1-z) - 2\right] + \left(\frac{11}{6}N_\mathrm{C} - \frac{2}{3}T_\mathrm{R}\right)\delta(1-z), \\
P_{q\leftarrow g}(z) &= \frac{1}{2}\left(z^2 + (1-z)^2\right).
\end{aligned} \tag{3.4}$$

The distribution $1/(1-z)_+$ is defined by

$$\int_0^1 \mathrm{d}z \frac{f(z)}{(1-z)_+} = \int_0^1 \mathrm{d}z \frac{f(z)-f(1)}{1-z}. \tag{3.5}$$

The definition of the non-singular part $C_{i\leftarrow j}$ of Eq. (3.3) is undetermined, however, and reflects a freedom of choice in the definition of the structure functions. For our analytic calculations, we have chosen the $\overline{\mathrm{MS}}$ factorization scheme defined by

$$C_{i\leftarrow j}^{\overline{\mathrm{MS}}} = 0. \tag{3.6}$$

STEP 3. Calculate the factorized cross-section $d\tilde{\sigma}$. It is given at order α_s^2 by:

$$
\begin{aligned}
\frac{s\ \mathrm{d}\tilde{\sigma}_{ij}}{\mathrm{d}t\ \mathrm{d}u} = \frac{s\ \mathrm{d}\sigma_{ij}}{\mathrm{d}t\ \mathrm{d}u} \\
& - \frac{\alpha_s}{2\pi}\sum_k \int_0^1 \mathrm{d}z_1\ R_{k\leftarrow i}(z_1,M^2)\ \frac{s\mathrm{d}\sigma_{kj}^{(1)}}{\mathrm{d}t}\bigg|_{p_1\to z_1p_1} \delta(z_1(s+t-Q^2)+u) \\
& - \frac{\alpha_s}{2\pi}\sum_k \int_0^1 \mathrm{d}z_2\ R_{k\leftarrow j}(z_2,M^2)\ \frac{s\mathrm{d}\sigma_{ik}^{(1)}}{\mathrm{d}t}\bigg|_{p_2\to z_2p_2} \delta(z_2(s+u-Q^2)+t).
\end{aligned}
\tag{3.7}
$$

The z_1 and z_2 integrals are trivial.

STEP 4. The two-jet collinear divergences will be associated with the limit $s_2 \to 0$ and will appear as inverse powers such as $s_2^{-1-\epsilon}$. Such terms will cause divergences when the x_1 and x_2 integrals are performed. These poles may be made manifest by using the identity:

$$
\frac{1}{(s_2)^{1+\epsilon}} = -\frac{1}{\epsilon}\delta(s_2)\left[1-\epsilon\ln A+\frac{1}{2}\epsilon^2\ln^2 A\right]+\frac{1}{(s_2)_{A+}}-\epsilon\left(\frac{\ln s_2}{s_2}\right)_{A+}+\mathrm{O}(\epsilon^2).
\tag{3.8}
$$

The poles will now all cancel explicitly between all collinear divergences, the virtual diagrams, and the factorization pieces. The results of this step are given in Appendix A.

STEP 5. Now that the poles are gone, we have an expression that can be evaluated numerically. We are ready to convolve $\mathrm{d}\tilde{\sigma}$ with the structure functions to compute the hadronic cross-section $\mathrm{d}\sigma/\mathrm{d}q_T^2\mathrm{d}y$. For the sake of evaluating distributions such as $1/(s_2)_{A+}$, it is convenient to rewrite the x_1 and x_2 integrals as[2,8]

$$
\begin{aligned}
\int_0^1 \mathrm{d}x_1 \int_0^1 \mathrm{d}x_2\theta(s_2) \to & \int_{\sqrt{T_+}e^y}^1 \frac{\mathrm{d}x_1}{(x_1S+T-Q^2)} \int_0^{A_1} \mathrm{d}s_2 \\
& + \int_{\sqrt{T_+}e^{-y}}^1 \frac{\mathrm{d}x_2}{(x_2S+T-Q^2)} \int_0^{A_2} \mathrm{d}s_2
\end{aligned}
\tag{3.9}
$$

where

$$A_1 = U + x_1(S + T - Q^2), \tag{3.10}$$

$$A_2 = \sqrt{\tau_+} e^y (x_2 S + T - Q^2) + Q^2 + x_2(U - Q^2), \tag{3.11}$$

$$\sqrt{\tau_+} = \sqrt{\frac{Q^2 + q_T^2}{S}} + \sqrt{\frac{q_T^2}{S}}. \tag{3.12}$$

4. Factorization Schemes

For the analytic results displayed in Appendix A, we used $\overline{\text{MS}}$ factorization. But one may make contact with any factorization scheme simply by adding the correction terms determined by Eq. (3.7):

$$\begin{aligned}\frac{s\ \mathrm{d}\tilde{\sigma}_{ij}}{\mathrm{d}t\ \mathrm{d}u} =& \frac{s\ \mathrm{d}\tilde{\sigma}_{ij}^{\overline{\text{MS}}}}{\mathrm{d}t\ \mathrm{d}u} \\ & - \frac{\alpha_s}{2\pi} \frac{1}{(s+t-Q^2)} C_{k\leftarrow i}\left(\frac{-u}{s+t-Q^2}, M^2\right) \left.\frac{s \mathrm{d}\sigma_{kj}^{(1)}}{\mathrm{d}t}\right|_{p_1 \to -up_1/(s+t-Q^2)} \\ & - \frac{\alpha_s}{2\pi} \frac{1}{(s+u-Q^2)} C_{k\leftarrow j}\left(\frac{-t}{s+u-Q^2}, M^2\right) \left.\frac{s \mathrm{d}\sigma_{ik}^{(1)}}{\mathrm{d}t}\right|_{p_2 \to -tp_2/(s+u-Q^2)}\end{aligned} \tag{4.1}$$

In particular, for our numeric work we have used the structure functions of Diemoz, Ferroni, Longo, and Martinelli.[9] They define the quark structure functions from deep inelastic scattering so that

$$xF_2(x, Q^2) = x\left[f_q(x, Q^2) + f_{\bar{q}}(x, Q^2)\right]. \tag{4.2}$$

This choice determines[10]

$$\begin{aligned} C_{q\leftarrow q}(z) =& C_{\rm F}\Bigg[(1+z^2)\left(\frac{\ln(1-z)}{1-z}\right)_+ - \frac{3}{2}\frac{1}{(1-z)_+} - \frac{1+z^2}{1-z}\ln z \\ &+ 3 + 2z - \left(\frac{9}{2}+\frac{1}{3}\pi^2\right)\delta(1-z)\Bigg], \\ C_{q\leftarrow g}(z) =& \frac{1}{2}\left[\left(z^2+(1-z)^2\right)\ln\left(\frac{1-z}{z}\right) + 6z(1-z)\right]. \end{aligned} \tag{4.3}$$

For the remaining coefficients, Diemoz *et. al.* take the simplest choice which enforces momentum conservation:

$$C_{g\leftarrow q}(z) = -C_{q\leftarrow q}(z) \qquad C_{g\leftarrow g}(z) = -4T_{\rm R}C_{q\leftarrow g}(z). \tag{4.4}$$

In the preceeding, the subscript q represents a single flavor of quark and the coefficient functions are defined identically for anti-quarks.

To integrate Eq. (4.1) as in Step 5, one may transform the distributions in z to the variable s_2 using the following identities:

$$z_1 \equiv \frac{-u}{s+t-Q^2}, \tag{4.5}$$

$$\delta(1-z_1) = (s_2-u)\delta(s_2), \tag{4.6}$$

$$\frac{1}{(1-z_1)_+} = (s_2-u)\left[\frac{1}{(s_2)_{A+}} + \delta(s_2)\ln\left|\frac{A}{u}\right|\right], \tag{4.7}$$

$$\begin{aligned} \left(\frac{\ln(1-z_1)}{1-z_1}\right)_+ =& (s_2-u)\Bigg[\left(\frac{\ln s_2}{s_2}\right)_{A+} - \frac{1}{(s_2)_{A+}}\ln(s_2-u) \\ &+ \frac{1}{2}\delta(s_2)\ln^2\left|\frac{A}{u}\right|\Bigg]. \end{aligned} \tag{4.8}$$

The remaining relations come from taking $z_1 \leftrightarrow z_2$ and $u \leftrightarrow t$ in the above.

5. Regularization of γ_5

The implementation of γ_5 in dimensional regularization is subtle and problematical. The technique we choose is completely straightforward to implement calculationally, but the underlying assumptions should be carefully laid out. We shall make a simple definition following Chanowitz *et. al.*[11] in cases where we have traces involving an even number of γ_5's. In the cases we have involving an odd number, the extension of the Dirac algebra from 4 to d dimensions will be shown to be irrelevant, and we will simply evaluate the traces in 4 dimensions.

From Chanowitz *et. al.*, we assume the following properties of γ_5:

(1) γ_5 anticommutes with all γ^μ in d dimensions,

(2) $\gamma_5^2 = 1$,

(3) $\mathrm{tr}(\gamma_5\gamma^\mu\gamma^\nu\gamma^\rho\gamma^\tau) = 4i\epsilon^{\mu\nu\rho\tau} \ + \ \mathrm{O}(d-4) \times$ ambiguity
on the four-dimensional subspace $\mu, \nu, \rho, \tau = 0, 1, 2, 3$,

and we assume

(4) $\mathrm{tr}(\gamma_5\gamma^\mu\gamma^\nu\gamma^\rho\gamma^\tau)$ is anti-symmetric.

The anomaly is intimately related to the fact that the ambiguous term above cannot be explicitly defined. In our calculation, however, this term will never be relevant.

Let us now consider squared amplitudes where each fermion loop connects to an even number of W's. For example, consider $|\mathrm{G}_2|^2$ shown in Figure 6. Each W vertex has vectorial and axial contributions. We first argue that the VA terms of the squared amplitude do not contribute. This is because the Dirac traces will all have one factor of $\mathrm{tr}(\gamma_5\gamma^\mu\gamma^\nu\gamma^\rho\gamma^\tau)$. Once we have performed the phase space integrals over p_3 and p_4, only three vectors remain: p_1, p_2, and q. But there is no non-zero contraction of three vectors with the anti-symmetric $\mathrm{tr}(\gamma_5\gamma^\mu\gamma^\nu\gamma^\rho\gamma^\tau)$. So the VA terms vanish once integrated over the phase space of the final partons.

In the limit of massless fermions, the AA terms are identical to the VV terms because one γ_5 can be anticommuted to the other and removed with $\gamma_5^2 = 1$. We can therefore treat W's as photons if we use the effective coupling constant:

$$g^2 \equiv g_V^2 + g_A^2. \tag{5.1}$$

The only interferences that involve fermion loops connected to an odd number of W's and that do not vanish are $2\mathrm{Re}(F_5 + F_6)^*(F_7 + F_8)$ and its brothers $2\mathrm{Re}(H_1 + H_2)^*(H_3 + H_4)$ and $2\mathrm{Re}(H_5 + H_6)^*(H_7 + H_8)$. In neither case is there any divergence when we do the momentum integrals; the regularization does not matter and we can do the traces unambiguously in 4 dimensions. To show this, it is not enough to know that the resulting answer is in fact finite. A trace of order $4-d$ could multiply a divergent integral that gave $1/(4-d)$. If we took the limit $d \to 4$ *before* doing the integral, we would falsely conclude that the result was zero. We must verify that this does not occur.

We use an argument by J.C. Collins[12] to show that the coefficient of possible divergences is *exactly* zero for any d near 4. Consider $2\mathrm{Re}(F_6^* F_8)$. There are two ways to route the large q_T of the W as shown in Figure 7. Divergences can arise when the other lines have small transverse momentum and correspond to potential collinear singularities of the gluons. In the first routing, the left gluon can become collinear with p_2 and p_4. The only unsuppressed gluon polarization ϵ^- is then parallel to its momentum k. In this limit, the gluon's upper vertex may be rewritten as $\epsilon^- \cdot \Gamma = k \cdot \Gamma / \left|\vec{k}\right|$. $k \cdot \Gamma$ is in a form where we can apply a Ward identity; it must cancel as shown in Figure 8.[13] Therefore, our potential divergence must cancel against the similar one of $2\mathrm{Re}(F_5^* F_8)$ shown in Figure 9. In a similar way, all divergences of $2\mathrm{Re}(F_5 + F_6)^*(F_7 + F_8)$ must pair up and cancel. This argument does not rely on d being exactly 4 and is independent of the nature of the W vertex and the precise definition of γ_5.

To conclude this section, we note that it would be nice to check the entire calculation by repeating it with an explicit definition of γ_5 in d dimensions such as $i\gamma_0\gamma_1\gamma_2\gamma_3$.[14] Such a definition avoids the ambiguity of $\mathrm{tr}(\gamma_5\gamma^\mu\gamma^\nu\gamma^\rho\gamma^\tau)$ but no longer anticommutes with all of the γ^μ. The calculation becomes more difficult computationally, and we have not attempted it.

6. Numerical Techniques and Results

The $dx\, ds_2$ integrands of Eq. (3.9) are in fact quite peaked at low values of x and s_2. To numerically integrate in a reasonable amount of time, it behooves us to transform to new variables that smooth out the integrand. The peak in s_2 occurs around $s_2 \sim q_T^2$ and the peak in the outer x integration around $\sqrt{q_T^2/S}$ above its lower limit $x_{min} = e^{\pm y}\sqrt{\tau_+}$. The integrand is smoothed out by changing variables to

$$\xi = \ln\left((x - x_{min}) + \epsilon\sqrt{q_T^2/S}\right), \tag{6.1}$$

$$\zeta = \ln\left(s_2 + \epsilon q_T^2\right). \tag{6.2}$$

By trial and error, $\epsilon = 0.1$ gives good convergence.

We will be working with five flavors and ignore the top quark. Correspondingly, we evolve $\alpha_s(M^2)$ using $N_f = 5$ in

$$\frac{d\alpha_s}{d(\ln M^2)} = -\frac{\beta_0}{4\pi}\alpha_s^2 - \frac{\beta_1}{16\pi^2}\alpha_s^3 \tag{6.3}$$

where

$$\beta_0 = 11 - \frac{2}{3}N_f, \qquad \beta_1 = 102 - \frac{38}{3}N_f. \tag{6.4}$$

For Λ_{QCD}, calculated with five flavors, we will consider 100, 175, and 250 MeV, which match to four-flavor values of 160, 260, and 360 Mev at the b threshold. When not otherwise indicated, we will in particular use the middle value of $\Lambda(4\text{ flavors}) = 260$ MeV.

We have chosen the renormalization scale μ^2 of the constituent cross-section to be the same as the factorization scale M^2 of the structure functions. We will examine M^2 at both of the physical scales of the problem: Q^2 and q_T^2. The sensitivity to this choice will help give us an error estimate for the calculation.

Finally, our particular choices of weak parameters are:

$$M_W = 81.8 \text{ GeV}, \qquad M_Z = 92.6 \text{ GeV} \tag{6.5}$$

$$\sin^2\theta_w = 1 - \frac{M_W^2}{M_Z^2}, \qquad \sin\theta_c = 0.219. \tag{6.6}$$

The results of all this machinery are shown in Fig. 10 for W^+ and Z production at the Tevatron. We have normalized the differential cross-sections with respect to the total cross-sections. The analytic form of the total cross-sections are known to first non-leading order,[15] and we have convolved with the Diemoz *et. al.* structure functions that we use for the rest of our computation.* For the factorization scale $M^2 = Q^2$ and Λ(4 flavors) = 260 MeV, these cross-sections are:

$$\sigma(W^+) = 9.68 \text{ nb}, \quad \sigma(Z) = 6.05 \text{ nb} \qquad \text{for } \sqrt{s} = 1.8 \text{ TeV}, \; M^2 = Q^2 \tag{6.7}$$

$$\sigma(W^+) = 2.80 \text{ nb}, \quad \sigma(Z) = 1.78 \text{ nb} \qquad \text{for } \sqrt{s} = 630 \text{ GeV}, \; M^2 = Q^2 \tag{6.8}$$

For contact with previous work, we show the predictions along with experimental data[16] for SPS energies in Fig. 11. But the data is not yet very sensitive to the size of the second-order contributions. Indeed, on the large logarithmic scale of these graphs, little difference between the first and second order calculations could be seen, and so these graphs are not very informative about our

---

⋆ Consistent with our coupling constant definitions in Appendix B, we have used weak coupling of $\alpha_w = \sqrt{2}G_F M_W^2/\pi$. Note that the exact choice of normalization cancels in the ratio $d\sigma/dq_T/q_T/\sigma$.

calculation. We have instead tabulated our results in Tables 1 and 2. Results are given for the choices $M^2 = Q^2$ and $M^2 = q_T^2$ of factorization scale. In the latter case, we have evaluated the total cross-section at $M^2 = \langle q_T^2 \rangle$. This scale is roughly (20 GeV)^2 at the Tevatron and (10 GeV)^2 at the SPS.[17]

$$\sigma(W^+) = 9.54 \text{ nb}, \quad \sigma(Z) = 6.13 \text{ nb} \qquad \text{for } \sqrt{s} = 1.8 \text{ TeV}, \; M^2 = (20 \text{ GeV})^2 \tag{6.9}$$

$$\sigma(W^+) = 3.80 \text{ nb}, \quad \sigma(Z) = 2.56 \text{ nb} \qquad \text{for } \sqrt{s} = 630 \text{ GeV}, \; M^2 = (10 \text{ GeV})^2 \tag{6.10}$$

Our results are given for q_T down to 20 GeV. This is roughly where the need for resummation becomes important as resummed first-order results become equal to first-order perturbative results.[17]

To show the second-order results visually, Figure 12 displays the K-factor: the ratio of the total of first and second order contributions to the first alone. Though convenient to plot, the K-factor is unphysical and sensitive to the choice of scale. Here, our convention is to normalize with respect to the first order cross-section at $M^2 = Q^2$. In this graph, one can see the difference between the choice of scale $M^2 = Q^2$ and $M^2 = q_T^2$ for the full second-order cross-section.

Fig. 13 explores more deeply the dependence on the choice of scale by plotting the results vs. M for a fixed choice of q_T. It is clear that the second order contribution helps stabilize the first order one, making it less sensitive to the choice of scale. There are two scales here which are sometimes attached favored status in the literature: the scale where the second order correction is zero and the scale where the total turns over. Looking at a smaller value of q_T in Fig. 14, however, both of these scales disappear. Numerically, the contribution of $gg \to q\bar{q}W$ is what keeps the second order correction positive here at small M. In our opinion, the most straightforward thing to do is to focus on the physical scales q_T^2 and Q^2 and use the discrepancy between them to estimate the error. Note that Figures 13 and 14 also show the sensitivity of the results to Λ_{QCD}.

There are four sources of theoretical error: the choice of renormalization scale that minimizes higher-order corrections, the value of Λ_{QCD}, the parametrization of the structure functions, and the growing need for resummation at small q_T. We have addressed the first two by examining the variation when Λ(4 flavors) = 160, 260, and 360 and $M^2 = Q^2$, q_T^2. For the Tevatron, the variation at the low q_T and high q_T ends of our results is roughly $\pm 10\%$ relative to the mean of the $M^2 = Q^2$ and $M^2 = q_T^2$ values listed in Table 1. We have taken this error for the entire range, giving the band drawn in Figure 10. This is not an extremely conservative estimate as only some sources of error can be addressed. However, it would be surprising if the true error were more than double this estimate.

For the SPS, we find a variation of roughly $\pm 10\%$ at the low q_T end and $\pm 35\%$ at the high q_T end. We have extrapolated for intermediate q_T to get the band of Figure 11. It is worth noting that taking the ratio of $d\sigma/dq_T^2$ with σ improved the error for low q_T and aggravated it for high q_T: the variations in $d\sigma/dq_T^2$ alone were roughly $\pm 15\%$ and $\pm 20\%$ respectively. For the Tevatron, taking the ratio changed the variation only slightly.

Finally, to give the reader a feel for the numerical contributions of different processes, we show their relative contribution at $M^2 = Q^2$ in Figs. 15 and 16.

Acknowledgements: We are greatly indebted to Keith Ellis for his advice and help in this project. Many analytic results for generic integrals were obtained from him and checked by us numerically. We would also like to thank John Collins for useful discussions and for the argument concerning γ_5 explained in the text.

APPENDIX A

In this appendix, we display the analytical results for $s d\sigma/dt du$ for the various processes of interest. $\overline{\mathrm{MS}}$ factorization has been used with dimensional regularization in $4 - 2\epsilon$ dimensions.

For notational simplicity, the results are given for massive photon production rather than directly for W and Z production. e_{f} is the appropriate fermion charge of $+\frac{2}{3}$ or $-\frac{1}{3}$. e_{f}^2 is slightly loose notation for the product of the two fermion charges relevant to the diagram at hand. With the exception of $2(\mathrm{F}_5 + \mathrm{F}_6)^*(\mathrm{F}_7 + \mathrm{F}_8)$, all of the diagrams calculated give identical results for axial and vectorial photons. For the exception, the different results are labelled by the superscripts (A) and (V).

Not all interference terms are listed. Having performed the phase-space integral on the final particles accompanying the photon, there are some simple relations. Interchanging $u \leftrightarrow t$ in the results will take

$$\mathrm{F}_1, \mathrm{F}_3, \mathrm{F}_5, \mathrm{F}_6 \leftrightarrow \mathrm{F}_2, \mathrm{F}_4, \mathrm{F}_7, \mathrm{F}_8 \qquad \mathrm{H}_1, \mathrm{H}_2, \mathrm{H}_5, \mathrm{H}_6 \leftrightarrow \mathrm{H}_3, \mathrm{H}_4, \mathrm{H}_7, \mathrm{H}_8. \tag{A.1}$$

Recall that diagrams H_5 through H_8 should not be included if both the two initial quarks and the two final quarks are identical. For non-identical final quarks, some of the H's are related to the F's by:

$$|\mathrm{H}_1 + \mathrm{H}_2|^2 = |\mathrm{H}_5 + \mathrm{H}_6|^2 = |\mathrm{F}_5 + \mathrm{F}_6|^2 ,$$

$$2(\mathrm{H}_1 + \mathrm{H}_2)^*(\mathrm{H}_3 + \mathrm{H}_4) = 2(\mathrm{F}_5 + \mathrm{F}_6)^*(\mathrm{F}_7 + \mathrm{F}_8). \tag{A.2}$$

For identical final quarks, the H combinations will be smaller than the F combinations by the symmetry factor $\frac{1}{2}$. Finally, we have the relation

$$2(\mathrm{F}_1^{(\mathrm{V})} + \mathrm{F}_2^{(\mathrm{V})})^*(\mathrm{F}_3^{(\mathrm{V})} + \mathrm{F}_4^{(\mathrm{V})}) = 0.$$

$2(\mathrm{F}_1 + \mathrm{F}_2)^*(\mathrm{F}_3 + \mathrm{F}_4)$ is zero for vectorial photons, W bosons, and Z bosons. The squared diagram has a loop of the final fermions connected to three gauge bosons: two gluons and the photon. Any vectorial contribution will vanish by Furry's Theorem. For W's and Z's, the axial contribution is proportional to $\mathrm{tr}\tau = 0$ and so also vanishes.

We will now present the results associated with the various terms of the squared diagrams. Many of the results for the F and H diagrams have already been presented by Ellis, *et. al.* Unfortunately, though they give exactly the combinations relevant to photon production, their expressions sum too many terms to be applied to W production. (See Appendix B.) We have recalculated these processes in the relevant combinations.

We will make use of the following definitions:

$$\mathcal{K} = 2\pi\alpha N_{\mathrm{C}} C_{\mathrm{F}} \frac{(1-\epsilon)}{\Gamma(1-\epsilon)} \left(\frac{4\pi\mu^2}{Q^2}\right)^{\epsilon} \left(\frac{sQ^2}{ut}\right)^{\epsilon} \tag{A.3}$$

$$K_{qq} = \frac{\mathcal{K}}{N_{\mathrm{C}}^2}, \quad K_{qg} = \frac{\mathcal{K}}{N_{\mathrm{C}}(2N_{\mathrm{C}}C_{\mathrm{F}})}, \quad K_{gg} = \frac{\mathcal{K}}{(2N_{\mathrm{C}}C_{\mathrm{F}})^2} \tag{A.4}$$

$$\lambda^2 = (u+t)^2 - 4s_2Q^2 \tag{A.5}$$

$$\mathcal{T}_0(Q^2,u,t) = \left[(1-\epsilon)\left(\frac{u}{t}+\frac{t}{u}\right) + \frac{2Q^2(Q^2-u-t)}{ut} - 2\epsilon\right]. \tag{A.6}$$

$\mathcal{T}_0(Q^2,u,t)$ is proportional to the squared matrix element for the lowest order process for $q\bar{q} \to g\gamma^*$.

A.1. The diagrams $\left|\sum_{i=1}^{2} L_i + \sum_{i=1}^{11} V_i\right|^2$

For $q\bar{q}$ scattering, the result is taken directly from Ellis, *et. al.*[2] The corresponding result for qg can be obtained by analytic continuation. The continuation is not completely trivial as one must take care with the branches of the logarithms that arise in the second-order cross-term $2\mathrm{Re}\left[\left(\sum_{i=1}^{2} L_i\right)^* \left(\sum_{i=1}^{11} V_i\right)\right]$. These logarithms yield terms like $i\pi$ when continued. If the result were calculated in

Euclidean space, where it is real, and continued to Minkowski space, unsquared $i\pi$'s would be dropped when we took the real part at the end. Keeping this in mind, it is possible to reconstruct the original and analytic Euclidean expression. It is then safe to continue Euclidean s to Euclidean u and visa versa. Then we continue back to Minkowski space and finish by taking the real part.

The result for both processes can then be written in the following form to order α_s^2:

$$\left(\frac{s\ \mathrm{d}\sigma}{\mathrm{d}t}\right)_{q\bar{q}} = e_f^2 \frac{K_{qq}}{s}\ \alpha_s(M^2)\ \mathcal{S}(s,t,u,R_{st},R_{su},R_{tu}) \tag{A.7}$$

$$\left(\frac{s\ \mathrm{d}\sigma}{\mathrm{d}t}\right)_{qg} = -e_f^2 \frac{K_{qg}}{s}\ \alpha_s(M^2)\ \Bigg[\mathcal{S}(u,t,s,\tilde{R}_{ut},\tilde{R}_{us},\tilde{R}_{ts}) - \frac{\alpha_s}{2\pi} T_0(Q^2,s,t) C_{\mathrm{F}} \pi^2\Bigg] \tag{A.8}$$

$$
\begin{aligned}
S(s,t,u,R_{st},R_{su},R_{tu}) = T_0(Q^2,u,t)\Bigg\{ & 1 + \frac{\alpha_s}{2\pi}\frac{\Gamma(1-\epsilon)}{\Gamma(1-2\epsilon)}\left(\frac{4\pi\mu^2}{Q^2}\right)^{\epsilon} \\
& \times \left[-\frac{(2C_{\rm F}+N_{\rm C})}{\epsilon^2} - \frac{1}{\epsilon}\left(3C_{\rm F} - 2C_{\rm F}\ln\left|\frac{s}{Q^2}\right| + \frac{11}{6}N_{\rm C} + N_{\rm C}\ln\frac{sQ^2}{ut} - \frac{2}{3}T_{\rm R}\right)\right] \\
& + \frac{\alpha_s}{2\pi}\left[\frac{2}{3}\pi^2 C_{\rm F} - \frac{1}{6}N_{\rm C}\pi^2 - 8C_{\rm F} - C_{\rm F}\ln^2\left|\frac{s}{Q^2}\right|\right. \\
& \left. + \frac{1}{2}N_{\rm C}\left(\ln^2\left|\frac{s}{Q^2}\right| - \ln^2\left|\frac{ut}{Q^4}\right|\right) + \left(\frac{11}{6}N_{\rm C} - \frac{2}{3}T_{\rm R}\right)\ln\frac{M^2}{Q^2} + N_{\rm C}R_{tu}\right]\Bigg\} \\
& + \frac{\alpha_s}{2\pi}\Bigg\{ C_{\rm F}\left(\frac{s}{s+u} + \frac{s}{s+t} + \frac{s+t}{u} + \frac{s+u}{t}\right) \\
& + \ln\left|\frac{t}{Q^2}\right|\left(C_{\rm F}\frac{(4s^2+2st+4su+tu)}{(s+u)^2} + N_{\rm C}\frac{t}{(s+u)}\right) \\
& + \ln\left|\frac{u}{Q^2}\right|\left(C_{\rm F}\frac{(4s^2+2su+4st+tu)}{(s+t)^2} + N_{\rm C}\frac{u}{(s+t)}\right) \\
& + (2C_{\rm F} - N_{\rm C})\left(2\ln\left|\frac{s}{Q^2}\right|\left(\frac{s^2}{(t+u)^2} + \frac{2s}{(t+u)}\right) - \frac{Q^2(t^2+u^2)}{tu(t+u)}\right) \\
& - (2C_{\rm F} - N_{\rm C})\left(\frac{s^2+(s+u)^2}{ut}R_{st} + \frac{s^2+(s+t)^2}{ut}R_{su}\right)\Bigg\}
\end{aligned}
\tag{A.9}
$$

$$
R_{st} = R_1(s,t), \qquad R_{su} = R_1(s,u), \qquad R_{tu} = R_2(t,u) \tag{A.10}
$$

$$
\tilde{R}_{ut} = \ln\left|\frac{u}{Q^2}\right|\ln\left|\frac{t}{Q^2}\right| - \frac{\pi^2}{2} - R_2(t,u) \tag{A.11}
$$

$$
\tilde{R}_{us} = R_1(s,u) \tag{A.12}
$$

$$
\tilde{R}_{ts} = \ln\left(\frac{s}{Q^2}\right)\ln\left|\frac{t}{Q^2}\right| + \frac{\pi^2}{2} - R_1(s,t) \tag{A.13}
$$

$$
\begin{aligned}
R_1(s,t) = & \ln\left(\frac{s}{Q^2}\right)\ln\left(\frac{t}{Q^2-s}\right) + \frac{1}{2}\ln^2\frac{s}{Q^2} \\
& - \frac{1}{2}\ln^2\left(\frac{Q^2-t}{Q^2}\right) + {\rm Li}_2\left(\frac{Q^2}{s}\right) - {\rm Li}_2\left(\frac{Q^2}{Q^2-t}\right)
\end{aligned}
\tag{A.14}
$$

$$R_2(t,u) = \frac{1}{2}\ln^2\left(\frac{Q^2-t}{Q^2}\right) + \frac{1}{2}\ln^2\left(\frac{Q^2-u}{Q^2}\right) + \mathrm{Li}_2\left(\frac{Q^2}{Q^2-t}\right) + \mathrm{Li}_2\left(\frac{Q^2}{Q^2-u}\right) \tag{A.15}$$

Li_2 is the dilogarithm function:

$$\mathrm{Li}_2(x) = -\int_0^x \frac{\mathrm{d}z}{z}\ln(1-z). \tag{A.16}$$

The ultraviolet renormalization has been performed using $\overline{\mathrm{MS}}$ subtraction.

A.2. THE DIAGRAMS $\left|\sum_{i=1}^{8} G_i\right|^2 + |F_1+F_2|^2$ FOR $q\bar{q} \to \gamma^*$

For completeness, we reproduce this result from Ellis, *et. al.*[2] These are the diagrams which, for $q\bar{q}$ scattering, cancel the divergences of the previous one loop processes. The contribution of $|F_1 + \mathrm{F}_2|^2$ may be isolated by considering only the terms proportional to T_R below.

$$
\begin{aligned}
\frac{s\,\mathrm{d}\sigma}{\mathrm{d}t\,\mathrm{d}u} &= e_f^2\frac{K_{qq}}{s}\alpha_s\Bigg\{T_0(Q^2,u,t)\delta(s_2)\Bigg[\frac{\alpha_s}{2\pi}\frac{\Gamma(1-\epsilon)}{\Gamma(1-2\epsilon)}\Big(\frac{4\pi\mu^2}{Q^2}\Big)^{\epsilon}\\
&\times\Big[\frac{(2C_{\mathrm{F}}+N_{\mathrm{C}})}{\epsilon^2}+\frac{1}{\epsilon}\Big(3C_{\mathrm{F}}+2C_{\mathrm{F}}\ln\frac{Q^2}{s}+N_{\mathrm{C}}\ln\frac{Q^2 s}{ut}+\frac{11}{6}N_{\mathrm{C}}-\frac{2}{3}T_{\mathrm{R}}\Big)\Big]\\
&+\frac{\alpha_s}{2\pi}\Big[(\frac{11}{6}N_{\mathrm{C}}-\frac{2}{3}T_{\mathrm{R}})\ln\frac{Q^2}{A}+(\frac{67}{18}N_{\mathrm{C}}-\frac{10}{9}T_{\mathrm{R}})\\
&+N_{\mathrm{C}}\ln^2\frac{Q^2}{A}+2C_{\mathrm{F}}\ln\Big(\frac{ut}{A^2}\Big)\ln\Big(\frac{M^2}{Q^2}\Big)\\
&+(C_{\mathrm{F}}-\frac{1}{2}N_{\mathrm{C}})\Big(\frac{\pi^2}{3}+\ln^2\Big(\frac{A^2 s}{Q^2 ut}\Big)\Big)-3C_{\mathrm{F}}\ln\Big(\frac{M^2}{Q^2}\Big)\Big]\Bigg]+\frac{\alpha_s}{2\pi}T_0(Q^2,u,t)\\
&\times\Big[\frac{\frac{2}{3}T_{\mathrm{R}}-\frac{11}{6}N_{\mathrm{C}}}{(s_2)_{A+}}+\frac{2C_{\mathrm{F}}}{(s_2)_{A+}}\ln\Big(\frac{(ut-Q^2s_2)}{(u-s_2)(t-s_2)}\Big)+4C_{\mathrm{F}}\Big(\frac{\ln(s_2/M^2)}{s_2}\Big)_{A+}\\
&+(C_{\mathrm{F}}-\frac{1}{2}N_{\mathrm{C}})\Big(4\Big(\frac{\ln(s_2/A)}{s_2}\Big)_{A+}+\frac{2}{(s_2)_{A+}}\ln\Big(\frac{s^2A^2}{(u-s_2)(t-s_2)(ut-Q^2s_2)}\Big)\Big)\Big]\Bigg\}\\
&+e_f^2\frac{K}{s}\frac{\alpha_s^2}{2\pi}\Bigg\{C_{\mathrm{F}}\Big[\frac{s}{(t-s_2)^2}-\frac{2}{(t-s_2)}-\frac{s}{ut}+\frac{(2Q^2u+ts_2-2Q^2s_2)}{t(ut-Q^2s_2)}+\frac{2Q^2(t-u)}{ut(t-s_2)}\Big]\\
&+N_{\mathrm{C}}\Big[-\frac{11}{6}\frac{(s+Q^2)}{ut}+\frac{s^2(3s_2-4t)}{2ut(t-s_2)^2}-\frac{2s}{u(t-s_2)}+\frac{Q^2}{3t^2}\Big]+T_{\mathrm{R}}\Big[\frac{2}{3}\frac{(s+Q^2)}{ut}-\frac{2}{3}\frac{Q^2}{t^2}\Big]\\
&+2(C_{\mathrm{F}}-\frac{1}{2}N_{\mathrm{C}})\ln\Big(\frac{ss_2}{ut-Q^2s_2}\Big)\Big[\frac{(Q^2-u)^2}{u(u-s_2)(t-s_2)}+\frac{(Q^2-u)^2}{ut(t-s_2)}\Big]\\
&+2(C_{\mathrm{F}}-\frac{1}{2}N_{\mathrm{C}})\ln\Big(\frac{ss_2}{(u-s_2)(t-s_2)}\Big)\frac{(s+Q^2)}{ut}\\
&+C_{\mathrm{F}}\ln\Big(\frac{(ut-Q^2s_2)}{(u-s_2)(t-s_2)}\Big)\Big[\frac{4Q^2(Q^2-t)^2}{ut(ut-Q^2s_2)}+\frac{2(Q^2+s)-s_2}{ut-Q^2s_2}+\frac{s_2-2s}{ut}\Big]\\
&+C_{\mathrm{F}}\ln\Big(\frac{M^2}{s_2}\Big)\Big[\frac{1}{ut(ut-Q^2s_2)}\Big[4ut(u-Q^2)-4Q^2(u-Q^2)^2-uts_2\Big]\\
&+\frac{Q^2-u}{(t-s_2)^2}+\frac{2Q^2-u}{t(t-s_2)}-\frac{2}{t}+\frac{Q^2}{t^2}\Big]\Bigg\}+e_f^2\frac{K}{s}\frac{\alpha_s^2}{2\pi}\{(u\leftrightarrow t)\}.
\end{aligned}
$$

A.3. The diagrams $\left|\sum_{i=1}^{8} G_i\right|^2$ for $qg \to \gamma^* qg$

$$\frac{s\ \mathrm{d}\sigma}{\mathrm{d}t\ \mathrm{d}u} = e_f^2 \frac{K_{qg}}{s} \frac{\alpha_s^2}{2\pi} [\mathcal{A}\delta(s_2) + \mathcal{B}N_\mathrm{C} + \mathcal{C}C_\mathrm{F}]$$

where

$$\begin{aligned}
\mathcal{A} = & \frac{\Gamma(1-\epsilon)}{\Gamma(1-2\epsilon)} \left(\frac{4\pi\mu^2}{Q^2}\right)^\epsilon [-T_0(Q^2,s,t)] \\
& \times \left\{ \frac{2C_\mathrm{F}+N_\mathrm{C}}{\epsilon^2} + \frac{1}{\epsilon}\left[3C_\mathrm{F} - 2C_\mathrm{F}\ln\left|\frac{u}{s}\right| + \frac{11}{6}N_\mathrm{C} + N_\mathrm{C}\ln\left(\frac{uQ^2}{st}\right) - \frac{2}{3}T_\mathrm{R}\right] \right. \\
& + N_\mathrm{C}\left[\frac{\pi^2}{6} + \frac{1}{2}\ln^2\left(\frac{sA^2}{utQ^2}\right)\right] + C_\mathrm{F}\left[\frac{7}{2} + \ln^2\left(\frac{A}{Q^2}\right) - \frac{3}{2}\ln\left(\frac{A}{Q^2}\right)\right] \\
& \left. + \left[\frac{11}{6}N_\mathrm{C} + \frac{3}{2}C_\mathrm{F} - \frac{2}{3}T_\mathrm{R} - 2N_\mathrm{C}\ln\left|\frac{t}{A}\right| - 2C_\mathrm{F}\ln\left|\frac{u}{A}\right|\right]\ln\left(\frac{Q^2}{M^2}\right)\right\}
\end{aligned}$$

$$
\begin{aligned}
\mathcal{B} = {} & \frac{s-t}{t(s_2-u)} - \frac{6st}{(s_2-t)^3} - \frac{3s+2u-7t}{t(s_2-t)} - \frac{9s+4u-4t}{(s_2-t)^2} + \frac{u-t}{t\lambda^2}(s_2+s) \\
& - \frac{3}{st^4}(ut-s_2Q^2)(t^2-4s_2Q^2) - \frac{(Q^2-t)^2}{st^2} - \frac{u(2u-Q^2)}{st^2} + \frac{s_2}{st} - \frac{1}{s} \\
& + \frac{u^2+(Q^2-t)^2}{s(s_2-t)}\left[\frac{1}{(s_2)_{A+}}\ln\left(\frac{sM^2}{ut-s_2Q^2}\right) - \left(\frac{\ln(s_2/M^2)}{s_2}\right)_{A+}\right] \\
& + \ln\left(\frac{sM^2}{(s_2-t)(s_2-u)}\right)\left[\frac{1}{s} + \frac{2}{(s_2)_{A+}} - \frac{(s_2+Q^2)^2+(s-Q^2)^2}{st(s_2)_{A+}}\right] \\
& + \ln\left(\frac{s_2}{M^2}\right)\left[\frac{4}{st(s_2-t)}\left(\frac{9}{4}u^2 - 2ut + 3su - 3st + s_2t + 2s^2\right) + \frac{2st}{(s_2-t)^3}\right. \\
& \left. + \frac{s_2(4u+6s)}{t(s_2-t)^2} + \frac{11}{2s} + \frac{s_2-4Q^2}{st} - \frac{10}{t} + \frac{2Q^2}{t^2}\right] \\
& - \left(\frac{\ln(s_2/M^2)}{s_2}\right)_{A+}\frac{1}{s}\left[\frac{1}{2t}(7(u+t)^2+9(u+s)^2+4u^2) + \frac{u^2}{s_2-t}\right] \\
& + \ln\left(\frac{Q^2M^2(s_2-t)^2}{ss_2t^2}\right)\left[\frac{4s_2Q^2}{st^4}(ut-s_2Q^2) - 2\frac{s-Q^2}{t^2} - \frac{1}{t} - \frac{5}{2s}\right. \\
& \left. + \frac{3s_2+4Q^2}{st} - 2\frac{s_2^2+4Q^4}{st^2}\right] - \ln\left(\frac{Q^2(s_2-u)^2}{su^2}\right)\left[\frac{u^2+(s-Q^2)^2}{2st(s_2)_{A+}}\right] \\
& + \left[\frac{1}{(s_2)_{A+}}\ln\left(\frac{Q^2(s_2-t)^2}{st^2}\right) - \left(\frac{\ln(s_2/M^2)}{s_2}\right)_{A+}\right]\frac{(s-Q^2)^2+(t-Q^2)^2}{2st} \\
& - 2\ln\left(\frac{s_2(2Q^2-u)-Q^2t}{st}\right)\left[\frac{(s_2-Q^2)^2+(2Q^2-u)^2}{2st(s_2-t)}\right] \\
& + \frac{1}{2t\lambda}\ln\left(\frac{s+Q^2-s_2+\lambda}{s+Q^2-s_2-\lambda}\right)\left[4s+3u+2s_2+\frac{3Q^2}{s}(s_2+2s-Q^2) - \frac{u}{s}(s_2-Q^2)\right. \\
& \left. - \frac{u+t}{(s_2)_{A+}}(s+2u) - \frac{u-t}{\lambda^2}(s_2+s)(s+Q^2-s_2)\right]
\end{aligned}
$$

$$
\begin{aligned}
C = {} & \frac{2}{s}\ln\left(\frac{s_2(ut-s_2Q^2)}{M^2(s_2-t)(s_2-u)}\right)\left[4+2\frac{s-4Q^2}{t}\right.\\
& \left.+\frac{1}{ut-s_2Q^2}\left((2u-t)^2+s_2(s_2-u)+Q^2(4u-t)\right)\right]\\
& -\left[\frac{1}{(s_2)_{A+}}\ln\left(\frac{ut-s_2Q^2}{(s_2-t)(s_2-u)}\right)+\left(\frac{\ln(s_2/M^2)}{s_2}\right)_{A+}\right]\frac{2(ut+s_2Q^2)}{st(ut-s_2Q^2)}(u^2+(s+u)^2)\\
& +\frac{2}{st}\ln\left(\frac{u[s_2(2Q^2-u)-Q^2t]}{Q^2(ut-s_2Q^2)}\right)\left[2s_2-u-5Q^2-\frac{u^2+(s_2-u)^2}{Q^2-u}\right]\\
& +\frac{1}{s}\ln\left(\frac{Q^2(s_2-u)^2}{su^2}\right)\left[\frac{u^2+(u+t)^2}{t(s_2)_{A+}}-\frac{ut-s_2Q^2}{u^2}+\frac{2s_2-Q^2}{u}\right.\\
& \left.+\frac{3s-8Q^2}{t}-1\right]-2\left(\frac{\ln(s_2/M^2)}{s_2}\right)_{A+}\left[\frac{2u+t}{s}\right]\\
& -\ln\left(\frac{s_2}{M^2}\right)\left[\frac{t-3Q^2}{su}+\frac{s_2Q^2}{su^2}+\frac{2}{s_2-u}+\frac{2st}{(s_2-t)^3}-2\frac{u+t}{(s_2-t)^2}\right.\\
& \left.+\frac{u^2+3Q^4}{st(s_2-t)}+\frac{2s_2-4Q^2}{s(s_2-t)}+\frac{3u-13Q^2}{st}-\frac{1}{s}+\frac{4}{t}+\frac{2}{u}+\frac{Q^2}{t^2}\right]\\
& +\frac{1}{\lambda^3}\left[\ln\left(\frac{s+Q^2-s_2+\lambda}{s+Q^2-s_2-\lambda}\right)-\frac{2\lambda}{s+Q^2-s_2}\right]\left[\frac{3sQ^2}{2t\lambda^2}(u-t)^2(2s_2-u-t)\right.\\
& +\frac{s_2t}{s}(3s_2-u-t)+\frac{s_2^2}{st}(u-2s_2)(t-2s)+\frac{ss_2}{t}(7s_2-11s)\\
& +\frac{su}{2t}(3u-s-25s_2)+u(13s_2+9s)-7t(u+t)\\
& \left.+s_2\left(19t-18s_2+\frac{7}{2}s\right)+\frac{3}{2}s(s+t)\right]\\
& -\frac{1}{\lambda}\ln\left(\frac{s+Q^2-s_2+\lambda}{s+Q^2-s_2-\lambda}\right)\left[\frac{u+t}{st(s_2)_{A+}}(u^2+(u+t)^2)-\frac{2}{st}(Q^2(u-2s_2-3s)\right.\\
& \left.+5Q^4+s_2u-\frac{7}{2}su-2s^2+s_2^2)\right]\\
& +\frac{1}{st\lambda^2(s+Q^2-s_2)}\left[2u^2Q^4-2s_2^2Q^2(s_2+3Q^2)+3s_2uQ^2(2u-3s_2-Q^2)\right.\\
& \left.+s_2t(2s_2u+6Q^2u+3Q^2s_2+Q^4)\right]
\end{aligned}
$$

$$
\begin{aligned}
&+\frac{1}{s}\left[\frac{1}{(s_2)_{A+}}\left(\frac{(Q^2-u)^2}{2t}+\frac{Q^4}{t}+4u+3t+Q^2\right).\right.\\
&+\frac{1}{s+Q^2-s_2}\left(\frac{s_2}{t}(7s_2-8u)+5u+7t-16s_2\right)\\
&\left.+\frac{1}{2t}(16s_2-11u+13Q^2)-\frac{2s_2+Q^2}{u}+\frac{s_2Q^2}{u^2}-\frac{sQ^2}{2t^2}-12\right]\\
&-\frac{2s}{t(s_2-u)}+\frac{8s_2(Q^2-u)}{(s_2-t)^3}-\frac{s+4Q^2}{(s_2-t)^2}+\frac{u(u+s)}{s(s_2-t)}\left(\frac{3}{t}-\frac{2}{(s_2)_{A+}}\right)\\
&-\frac{u^2(3s_2+Q^2)}{st\lambda^2}+\frac{1}{s_2-t}\left(\frac{u}{(s_2)_{A+}}+\frac{3s_2-2u}{s}-\frac{s}{t}\right)\\
&+\frac{1}{ut-s_2Q^2}\left[s_2-t+\frac{4}{s}\left(\frac{Q^2}{t}\big(u(u+s)+t(t+s)\big)-\frac{Q^2ut}{(s_2)_{A+}}-u^2\right)\right]
\end{aligned}
$$

A.4. THE DIAGRAMS $\left|\sum_{i=1}^{8} G_i\right|^2$ FOR $gg \to \gamma^* q\bar{q}$

$$
\begin{aligned}
\frac{s\,\mathrm{d}\sigma}{\mathrm{d}t\,\mathrm{d}u} = e_f^2 \frac{K_{gg}}{s}\frac{\alpha_s^2}{2\pi}\Bigg\{ \Bigg[&\frac{2C_\mathrm{F}}{(s_2-u)(Q^2-u)}\Bigg(\frac{s_2^2 Q^4}{su^2}+\frac{s_2 Q^2}{u}-\frac{u^2+s_2^2}{s+Q^2-s_2} \\
&+\frac{u^2}{s}-s_2\Bigg) - N_\mathrm{C}\frac{u^2+(s+Q^2)^2}{s(s_2-u)(s+Q^2-s_2)}\Bigg] \ln\left(\frac{M^2Q^2(s_2-u)^2}{ss_2u^2}\right) \\
&+(2C_\mathrm{F}-N_\mathrm{C})\frac{s_2^2+(s-Q^2)^2}{s(s_2-t)(s_2-u)}\ln\left(\frac{ss_2^2}{M^2(s_2-t)(s_2-u)}\right) \\
&+\left(\frac{2C_\mathrm{F}}{Q^2-t}-\frac{N_\mathrm{C}}{s}\right)\frac{s_2^2+(t-2Q^2)^2}{(s_2-u)(s+Q^2-s_2)}\ln\left(\frac{s_2[s_2(2Q^2-t)-Q^2u]^2}{M^2sQ^2(s_2-u)^2}\right) \\
&+\Bigg[\frac{2C_\mathrm{F}}{ut-s_2Q^2}\Bigg(\frac{2s(s_2+2Q^2)}{s+Q^2-s_2}-\frac{4s_2(s_2+Q^2)}{s_2-u}-s_2-5Q^2 \\
&+\frac{4s_2^3(Q^2-s_2)}{(s_2-t)(s_2-u)(s+Q^2-s_2)}+2\frac{[s_2^2+(t-2Q^2)^2][s_2(2Q^2-t)-Q^2u]}{(Q^2-t)(s_2-u)(s+Q^2-s_2)}\Bigg) \\
&+N_\mathrm{C}\frac{u^2+t^2}{s(s_2-t)(s_2-u)}\Bigg]\ln\left(\frac{s_2(ut-s_2Q^2)}{M^2(s_2-t)(s_2-u)}\right) \\
&-\frac{8C_\mathrm{F}s_2}{(s_2-u)^2}\ln\frac{s_2}{M^2}+\frac{C_\mathrm{F}}{\lambda}\frac{4(2Q^2-s_2)}{(s+Q^2-s_2)}\ln\left(\frac{s+Q^2-s_2+\lambda}{s+Q^2-s_2-\lambda}\right) \\
&+\frac{N_\mathrm{C}}{\lambda}\Bigg[\frac{s_2(u-t)^2}{\lambda^4}\Bigg(\frac{4Q^2(Q^2-s)}{s+Q^2-s_2}-\frac{5s_2(Q^2-s_2)}{2s}+2s-8Q^2-\frac{9}{2}s_2\Bigg) \\
&+\frac{1}{\lambda^2}\Bigg(\frac{3(u^2-t^2)^2}{8s(s+Q^2-s_2)}+\frac{s_2+Q^2}{s+Q^2-s_2}(2ut-3s_2Q^2)+\frac{ut}{2s}(17s_2+3Q^2) \\
&+\frac{s_2^2}{2s}(s_2-21Q^2)+\frac{3}{2}ut-\frac{s_2}{4}(7u+7t+2s)\Bigg) \\
&+\frac{2(ut-5Q^4)}{s(s+Q^2-s_2)}-\frac{9(s_2+2Q^2)}{4(s+Q^2-s_2)}+\frac{3(s_2+7Q^2)}{8s}-\frac{27}{8}\Bigg]\ln\left(\frac{s+Q^2-s_2+\lambda}{s+Q^2-s_2-\lambda}\right) \\
&+2C_\mathrm{F}\left[\frac{1}{su^2}\left(s_2Q^2-\frac{(s_2^2+u^2)}{(s_2-u)^2}(ut-s_2Q^2)\right)-\frac{2s_2}{ut-s_2Q^2}\left(\frac{su}{(s_2-u)^2}+\frac{2Q^2}{s}\right)\right] \\
&+N_\mathrm{C}\left[\frac{8s_2}{(s_2-t)^2}-\frac{4(s_2-u)}{s(s_2-t)}+\frac{1}{s}-\frac{1}{s(s+Q^2-s_2)^2}\left(4ut+s_2s+(4s-3s_2)Q^2\right)\right] \\
&+\frac{N_\mathrm{C}}{\lambda^2(s+Q^2-s_2)^2}\Bigg[3s_2Q^2(u-t)^2\left(\frac{4(s+Q^2)}{\lambda^2}+\frac{1}{s}\right)+(3s_2+4Q^2)(u-t)^2 \\
&-4s_2Q^2(s+Q^2)\Bigg]\Bigg\} \;+\; e_f^2\frac{K_{gg}}{s}\frac{\alpha_s^2}{2\pi}\{u\leftrightarrow t\}
\end{aligned}
$$

A.5. The diagrams $2(\mathrm{F}_1 + \mathrm{F}_2)^*(\mathrm{F}_5 + \mathrm{F}_6)$

$$
\begin{aligned}
\frac{s\,\mathrm{d}\sigma}{\mathrm{d}t\,\mathrm{d}u} = & e_f^2 \frac{K_{qq}}{s}\frac{\alpha_s^2}{2\pi}(C_\mathrm{F} - \frac{1}{2}N_\mathrm{C})\frac{1}{ut} \\
& \times \Bigg\{ 2u - \frac{s^2 + 3uQ^2}{t} + \frac{s_2^2 s^2}{t(s_2 - t)^2} + \frac{(s+u)^2}{s_2} + \frac{s^2 t}{s_2(s_2 - t)} \\
& + \frac{2}{\lambda^2}(u^2 + ut + st)\left(2Q^2 - t + \frac{u}{s_2}(s - Q^2)\right) \\
& + \frac{u+t}{s+Q^2-s_2}\left[\frac{2s}{\lambda^2}\left(1 + 12\frac{sQ^2}{\lambda^2}\right)(ut - s_2Q^2) + \frac{(s_2-u)^2}{s_2} - \frac{4s^2u^2}{s_2\lambda^2}\right] \\
& + \frac{1}{s_2\lambda}\Bigg[u^2(s_2 + Q^2) - 2us_2Q^2 + \frac{s^2}{4}(5u + 17t) \\
& + 3stu + \frac{s}{\lambda^2}(u+t)\left(u(u^2 - t^2) - s(3t^2 - 2s_2Q^2)\right) \\
& + \frac{3s^2}{4\lambda^4}(u+t)(u^2 - t^2)^2\Bigg] \ln\left(\frac{s+Q^2-s_2+\lambda}{s+Q^2-s_2-\lambda}\right) \\
& + \left[\frac{2uQ^2}{t} - \frac{u^2 + 2s(s+u)}{s_2}\right] \ln\left(\frac{Q^2(s_2-t)^2}{st^2}\right) \Bigg\}
\end{aligned}
$$

The coefficient of $1/s_2$ is zero when $s_2 \to 0$; so $1/(s_2)_{A+}$ and $1/s_2$ are identical here.

A.6. The diagrams $2(\mathrm{F}_3 + \mathrm{F}_4)^*(\mathrm{F}_5 + \mathrm{F}_6)$

$$\frac{s\,\mathrm{d}\sigma}{\mathrm{d}t\,\mathrm{d}u} = e_f^2 \frac{K_{qq}}{s}\frac{\alpha_s^2}{2\pi}(C_\mathrm{F} - \frac{1}{2}N_\mathrm{C})$$

$$\times \Bigg\{ \frac{48}{\lambda^4}\frac{s s_2 Q^2(ut - s_2 Q^2)}{t(s+Q^2-s_2)} + \frac{2}{\lambda^2}\Bigg(-2\frac{[Q^2(s_2-u)^2 + 3s(t-2Q^2)^2]}{t(s+Q^2-s_2)}$$

$$+ \frac{1}{st}(s_2(s^2+Q^4) + 7sQ^2(s+Q^2) - s^3 - Q^6) + \frac{1}{s}(Q^2 + s_2^2 - 2s_2 u)$$

$$+ 2t - 5s - 8Q^2\Bigg) + \frac{2}{st}\Bigg(u + 2t + 2s_2 + Q^2 - \frac{2s_2Q^2}{t} + \frac{s_2(Q^2-u)}{s_2-t}$$

$$+ \frac{(s_2+t)^2 - 4Q^2(s+t)}{s+Q^2-s_2}\Bigg) - \frac{(s+Q^2)^2 - s_2^2}{st(s+Q^2-s_2)}\ln\left(\frac{Q^2(s_2-t)^2}{st^2}\right)$$

$$+ \frac{1}{\lambda}\Bigg[-\frac{24}{\lambda^4}\frac{s s_2 Q^2}{t}(ut - s_2Q^2) + \frac{2}{\lambda^2}\Bigg(\frac{s-Q^2}{s}(u-s_2)(s+s_2-Q^2)$$

$$+ \frac{u^2}{t}(Q^2 - s) - u(3s + 3s_2 - Q^2) - \frac{s_2}{t}(t^2 - 2s_2 t - 6sQ^2 + 2Q^4)\Bigg)$$

$$+ \frac{1}{st}\Bigg(\frac{2t}{s+Q^2-s_2}(2Q^2 t + s_2(4s - s_2 - t)) + (s_2 - u)^2$$

$$+ 3(s_2-t)^2 + 2s^2 + 2st - 4t^2\Bigg)\Bigg] \ln\left(\frac{s+Q^2-s_2+\lambda}{s+Q^2-s_2-\lambda}\right)$$

$$- 2\frac{(s_2-t)^2 + s_2^2}{st(s+Q^2-s_2)}\ln\left(\frac{s_2(2Q^2-u) - Q^2 t}{st}\right)\Bigg\}$$

A.7. THE DIAGRAMS $|\mathrm{F}_3 + \mathrm{F}_4|^2$

We have corrected two typographic mistakes in the result appearing in Ellis, *et. al.*The published version contained a sign mistake on the $2t$ term of the second line and a mistake in the overall group factor of C_F which should instead be $1/2$.

$$
\begin{aligned}
\frac{s\ \mathrm{d}\sigma}{\mathrm{d}t\ \mathrm{d}u} =& \sum\nolimits_f e_f^2 \frac{K_{qq}}{s}\frac{\alpha_s^2}{2\pi} \times \frac{1}{2}\Bigg\{ \frac{1}{2(s+Q^2-s_2)}\left(\frac{u}{s}-1\right) - \frac{5}{4s} \\
&+ \frac{1}{\lambda^2}\left[\frac{u}{s+Q^2-s_2}\left(-2s+\frac{3u}{2s}(t-u)+4u-2t\right)+\frac{u}{2s}(2s+2s_2+t-u)\right] \\
&+ \frac{3u^2(u-t)}{\lambda^4}\left[\frac{2s-u-t}{s+Q^2-s_2}-\frac{s+s_2}{s}\right] \\
&+ \frac{1}{\lambda}\ln\left(\frac{s+Q^2-s_2+\lambda}{s+Q^2-s_2-\lambda}\right)\left[\frac{1}{s+Q^2-s_2}\left(\frac{2u^2}{s}+\frac{5}{2}u+\frac{3}{2}s\right)+\frac{1}{s}(\frac{3}{4}s+u-\frac{1}{2}s_2)\right] \\
&+ \frac{1}{\lambda^3}\ln\left(\frac{s+Q^2-s_2+\lambda}{s+Q^2-s_2-\lambda}\right)\left[\frac{u^2}{s+Q^2-s_2}\left(3u-t-\frac{u^2}{s}+\frac{t^2}{s}-2s\right)\right. \\
&+ \left.\frac{u}{s}(2s_2t-ut-2s_2^2+4us_2-3u^2+2ss_2-us)\right] + \frac{1}{\lambda^5}\ln\left(\frac{s+Q^2-s_2+\lambda}{s+Q^2-s_2-\lambda}\right) \\
&\times \left[\frac{3(u^2-t^2)u^2}{s+Q^2-s_2}(s-Q^2)+\frac{3u^2Q^2}{s}(u-t)(u+t-2s_2)\right]\Bigg\} + \{(u\leftrightarrow t)\}
\end{aligned}
$$

A.8. THE DIAGRAMS $|\mathrm{F}_5+\mathrm{F}_6|^2$

$$
\begin{aligned}
\frac{s\ \mathrm{d}\sigma}{\mathrm{d}t\ \mathrm{d}u} =& e_f^2 \frac{K_{qq}}{s}\frac{\alpha_s^2}{2\pi} \\
&\times \frac{1}{2}\Bigg\{\left[2\frac{(s_2-u)}{t^2}\left(2\frac{s_2}{t}-1\right)^2 - 4\frac{s_2u}{t^3} - 2\frac{s}{t^2}\left(2\frac{s_2^2}{t^2}+1\right)\right. \\
&- \left.\frac{1}{s}\left(2\frac{s_2^2}{t^2}-2\frac{s_2}{t}+1\right)\left(2\left(\frac{s_2-u}{t}\right)^2-2\frac{(s_2-u)}{t}+1\right)\right] \\
&\times \left(3+\ln\left(\frac{M^2Q^2(s_2-t)^2}{ss_2t^2}\right)\right) + \left[\frac{s}{(s_2-t)^2}+2\frac{st+s_2Q^2}{t^2(s_2-t)}\right]\ln\left(\frac{s_2}{M^2}\right) \\
&+ \left[\frac{s(u^2-t^2)}{t\lambda^3}+\frac{2u+3s}{t\lambda}\right]\ln\left(\frac{s+Q^2-s_2+\lambda}{s+Q^2-s_2-\lambda}\right) + \frac{(u-t)(s+s_2-Q^2)}{t\lambda^2} \\
&+ 4\frac{s_2}{st}\left(\frac{s_2}{t}-1\right) + 6\frac{s_2-u}{st}\left(\frac{s_2-u}{t}-1\right) + \frac{3}{s} + \frac{9u+7s-5s_2}{t^2} \\
&+ \frac{u+t}{t(s_2-t)} - \frac{s}{(s_2-t)^2}\Bigg\}
\end{aligned}
$$

A.9. THE DIAGRAMS $2(\mathrm{F}_5^{(V)} + \mathrm{F}_6^{(V)})^*(\mathrm{F}_7^{(V)} + \mathrm{F}_8^{(V)})$

$$
\begin{aligned}
\frac{s\,\mathrm{d}\sigma}{\mathrm{d}t\,\mathrm{d}u} =& e_f^2 \frac{K_{qq}}{s}\frac{\alpha_s^2}{2\pi} \\
& \times \frac{1}{2}\left\{ \frac{s(s_2^2 - ut)}{ut(s_2-u)(s_2-t)} - \frac{u+t}{2ut} - \frac{(s+s_2-Q^2)(u-t)^2}{2ut\lambda^2} \right. \\
& + \frac{1}{\lambda}\left[\frac{(3s+2s_2)(u+t)}{2ut} + 2\frac{s-Q^2}{s+Q^2-s_2} - \frac{s(u+t)(u-t)^2}{2ut\lambda^2} \right] \\
& \times \ln\left(\frac{s+Q^2-s_2+\lambda}{s+Q^2-s_2-\lambda}\right) - \frac{Q^2\left[2(s_2-t)^2 + s_2^2 + s^2\right]}{ut(Q^2-u)(Q^2-t)} \ln\left(\frac{ut - s_2Q^2}{(s_2-u)(s_2-t)}\right) \\
& + \frac{(s_2-Q^2)^2 + (s_2-t)^2 + s_2^2 + s^2}{t(Q^2-u)(s+Q^2-s_2)} \ln\left(\frac{\left[s_2(2Q^2-u) - Q^2t\right]^2}{sQ^2(s_2-t)^2}\right) \\
& \left. - \frac{(2Q^2-t)\left[t^2 + 2(s_2^2 + s^2 - s_2t)\right]}{ut(Q^2-t)(s+Q^2-s_2)} \ln\left(\frac{Q^2(s_2-t)^2}{st^2}\right) \right\} \\
& + e_f^2 \frac{K_{qq}}{s}\frac{\alpha_s^2}{2\pi} \times \frac{1}{2}\{(u \leftrightarrow t)\}
\end{aligned}
$$

A.10. THE DIAGRAMS $2(\mathrm{F}_5^{(A)} + \mathrm{F}_6^{(A)})^*(\mathrm{F}_7^{(A)} + \mathrm{F}_8^{(A)})$

$$
\begin{aligned}
\frac{s\,\mathrm{d}\sigma}{\mathrm{d}t\,\mathrm{d}u} =& e_f^2 \frac{K_{qq}}{s}\frac{\alpha_s^2}{2\pi} \\
& \times \frac{1}{2}\left\{ \frac{s}{ut} - \frac{1}{t} + \frac{2s}{t(s_2-u)} + \frac{(u-2s_2)(u-t)}{t\lambda^2} \right. \\
& - \frac{s+s_2}{ut} \ln\left(\frac{Q^2(s_2-t)(s_2-u)}{stu}\right) \\
& + \frac{1}{\lambda}\left[\frac{3s+2s_2}{t} + \frac{2(s-u)}{s+Q^2-s_2} - \frac{s(u^2-t^2)}{t\lambda^2} - 1 \right] \ln\left(\frac{s+Q^2-s_2+\lambda}{s+Q^2-s_2-\lambda}\right) \\
& - \frac{2}{t(s+Q^2-s_2)}\left[2(Q^2-t) + \frac{u(u-2s_2)}{s+t-s_2} \right] \ln\left|\frac{u\left[s_2(2Q^2-u) - Q^2t\right]}{Q^2(ut - s_2Q^2)}\right| \\
& \left. + \frac{1}{ut}\left[Q^2 - 2s - \frac{u^2 + t^2 + 4s(u+t)}{s+Q^2-s_2} \right] \ln\left(\frac{Q^2(ut - s_2Q^2)}{stu}\right) \right\} \\
& + e_f^2 \frac{K_{qq}}{s}\frac{\alpha_s^2}{2\pi} \times \frac{1}{2}\{(u \leftrightarrow t)\}
\end{aligned}
$$

A.11. The diagrams $2(\mathrm{H}_1 + \mathrm{H}_2)^*(\mathrm{H}_5 + \mathrm{H}_6)$

$$
\begin{aligned}
\frac{s\, \mathrm{d}\sigma}{\mathrm{d}t\, \mathrm{d}u} =& e_f^2 \frac{K_{qq}}{s} \frac{\alpha_s^2}{2\pi} (C_\mathrm{F} - \frac{1}{2} N_\mathrm{C}) \frac{-4}{t} \\
& \times \left\{ \frac{Q^2}{t} \ln \left(\frac{Q^2 (s_2 - t)^2}{s t^2} \right) + \frac{(s_2 - Q^2)^2 + s^2}{(s_2 - t)(s + Q^2 - s_2)} \ln \left(\frac{s_2 (2Q^2 - u) - Q^2 t}{st} \right) \right\} \\
& \times \left\{ \text{ Factor of } \frac{1}{2} \text{ if identical final quarks. } \right\}
\end{aligned}
$$

A.12. The diagrams $2(\mathrm{H}_1 + \mathrm{H}_2)^*(\mathrm{H}_7 + \mathrm{H}_8)$

$$
\begin{aligned}
\frac{s\, \mathrm{d}\sigma}{\mathrm{d}t\, \mathrm{d}u} =& e_f^2 \frac{K_{qq}}{s} \frac{\alpha_s^2}{2\pi} (C_\mathrm{F} - \frac{1}{2} N_\mathrm{C}) \frac{2}{stu} \\
& \times \left\{ 2 s_2 Q^2 \frac{u^2 + t^2}{ut} - (u + t)^2 + \left[2 s_2 (Q^2 - s) - (u + t)^2 \right] \ln \left(\frac{Q^2 s_2}{ut} \right) \right\} \\
& \times \left\{ \text{ Factor of } \frac{1}{2} \text{ if identical final quarks. } \right\}
\end{aligned}
$$

APPENDIX B

In this appendix, we show explicitly how to adapt the formula of Appendix A to W and Z production. One must (1) include the flavor contractions and Cabbibo angles appropriate to each result; (2) use the appropriate weak coupling constants; and (3) sum over final flavors. The results are given below. One should use the formula of Appendix A ignoring e_f^2 and $\sum_f e_\mathrm{f}^2$ since charges and final flavor sums will be displayed explicitly below when relevant. For the proper overall normalization, α must be replaced by $\alpha_w/4$ which we take in terms of G_F

as

$$\alpha \to \frac{\alpha_w}{4} = \frac{\sqrt{2} G_F M_W^2}{4\pi} \tag{B.1}$$

Also, ignore any symmetry factors of $\frac{1}{2}$ mentioned in the formula of Appendix A as these are also displayed explicitly.

$$\begin{aligned}
u\bar{d} \to W^+ \ &: \ \Theta_{ij}\left[(q\bar{q} \to g\gamma^*) + (q\bar{q} \to gg\gamma^*) + 2T_{\mathrm{R}}\left|\mathrm{F}_1 + \mathrm{F}_2\right|^2\right] \\
&\quad + \left[U_{ii}\left|\mathrm{F}_5 + \mathrm{F}_6\right|^2 + D_{jj}(u \leftrightarrow t)\right] \\
&\quad + \Theta_{ij}\left[2(\mathrm{F}_1 + \mathrm{F}_2)^*(\mathrm{F}_5 + \mathrm{F}_6) + (u \leftrightarrow t)\right] \\
u\bar{u} \to W^+ \ &: \ (\mathrm{tr}D)\delta_{ij}\left|\mathrm{F}_3 + \mathrm{F}_4\right|^2 + U_{ii}\left|\mathrm{F}_5 + \mathrm{F}_6\right|^2 \\
&\quad + \delta_{ij}U_{ii}2(\mathrm{F}_3 + \mathrm{F}_4)^*(\mathrm{F}_5 + \mathrm{F}_6) \\
uu \to W^+ \ &: \ \left[U_{ii}\left|\mathrm{F}_5 + \mathrm{F}_6\right|^2 + U_{jj}(u \leftrightarrow t)\right] \\
&\quad + \delta_{ij}U_{ii}2(\mathrm{H}_1 + \mathrm{H}_2)^*(\mathrm{H}_7 + \mathrm{H}_8) \\
ud \to W^+ \ &: \ U_{ii}\left|\mathrm{F}_5 + \mathrm{F}_6\right|^2 + \frac{1}{2}\Theta_{ij}2(\mathrm{H}_1 + \mathrm{H}_2)^*(\mathrm{H}_5 + \mathrm{H}_6) \\
ug \to W^+ \ &: \ U_{ii}\left[(qg \to q\gamma^*) + (qg \to qg\gamma^*)\right] \\
gg \to W^+ \ &: \ (\mathrm{tr}D)(gg \to q\bar{q}\gamma^*) \\
\text{more} \ &: \ u \leftrightarrow \bar{d},\ d \leftrightarrow \bar{u},\ \Theta \leftrightarrow \Theta^T,\ \text{and } U \leftrightarrow D \\
&\quad \text{in all the above}
\end{aligned} \tag{B.2}$$

i and j are family indices of the colliding partons and are not to be implicitly summed above. The matricies

$$\Theta_{ij} = \left|K_{ij}\right|^2, \quad D_{ij} = \mathrm{Re}(K^\dagger K)_{ij}, \quad U_{ij} = \mathrm{Re}(KK^\dagger)_{ij} \tag{B.3}$$

contain the mixing angles. K is the KM matrix projected onto those particles for which we are above threshold. (In particular, $KK^\dagger$ is not necessarily the unit matrix.)

The symmetry which allows us to take $u \leftrightarrow \bar{d}$ as directed is a combination of CP, isospin, and a 180 degree rotation of the plane of the W and the beam (which is equivalent to P in that plane).

In our numerical work, we have included the flavors through b and ignored the t quark. We have also ignored terms of order

$$(b \text{ content of proton}) \times (b \text{ mixing angles})$$

and so have approximated

$$\Theta \simeq \begin{pmatrix} \cos^2\theta_c & \sin^2\theta_c & \\ \sin^2\theta_c & \cos^2\theta_c & \\ & & 0 \end{pmatrix}, \qquad D \simeq U \simeq \begin{pmatrix} 1 & & \\ & 1 & \\ & & 0 \end{pmatrix}. \tag{B.4}$$

For Z production, the combinations are:

$$\begin{aligned}
u\bar{d} \to Z \;&:\; \mathcal{A}_{ud} \\
u\bar{u} \to Z \;&:\; \delta_{ij} g_u^2 \left[(q\bar{q} \to g\gamma^*) + (q\bar{q} \to gg\gamma^*) + 2T_{\rm R} \left| {\rm F}_1 + {\rm F}_2 \right|^2 \right] \\
&\quad + \delta_{ij} g_u^2 \left[2({\rm F}_1 + {\rm F}_2 + {\rm F}_3 + {\rm F}_4)^* ({\rm F}_5 + {\rm F}_6) + (u \leftrightarrow t) \right] \\
&\quad + \delta_{ij} (N_u g_u^2 + N_d g_d^2) \left| {\rm F}_3 + {\rm F}_4 \right|^2 + \mathcal{A}_{uu} \\
ud \to Z \;&:\; \mathcal{A}_{ud} \\
uu \to Z \;&:\; \frac{1}{2} \delta_{ij} g_u^2 \left[2({\rm H}_1 + {\rm H}_2)^* ({\rm H}_5 + {\rm H}_6 + {\rm H}_7 + {\rm H}_8) + (u \leftrightarrow t) \right] \\
&\quad + \mathcal{A}_{uu} \\
ug \to Z \;&:\; g_u^2 \left[(qg \to q\gamma^*) + (qg \to qg\gamma^*) \right] \\
gg \to Z \;&:\; (N_u g_u^2 + N_d g_d^2)(gg \to q\bar{q}\gamma^*) \\
\text{more} \;&:\; u \leftrightarrow d \text{ above} \\
\text{more} \;&:\; u \leftrightarrow \bar{u} \text{ and } d \leftrightarrow \bar{d} \text{ above}
\end{aligned} \tag{B.5}$$

where

$$\begin{aligned}
\mathcal{A}_{ab} = &\left[g_a^2 \left| {\rm F}_5 + {\rm F}_6 \right|^2 + g_b^2 (u \leftrightarrow t) \right] \\
&+ g_a^{({\rm V})} g_b^{({\rm V})} 2({\rm F}_5^{({\rm V})} + {\rm F}_6^{({\rm V})})^* ({\rm F}_7^{({\rm V})} + {\rm F}_8^{({\rm V})}) \\
&+ g_a^{({\rm A})} g_b^{({\rm A})} 2({\rm F}_5^{({\rm A})} + {\rm F}_6^{({\rm A})})^* ({\rm F}_7^{({\rm A})} + {\rm F}_8^{({\rm A})})
\end{aligned} \tag{B.6}.$$

N_u and N_d are the number of up and down flavors for which we are above threshold. The effective charges are

$$
\begin{aligned}
g^{(\mathrm{V})} &= \left(\frac{M_W^2}{4M_Z^2}\right)^{\frac{1}{2}} (\tau_3 - 4Q\sin^2\theta_W), \\
g^{(\mathrm{A})} &= \left(\frac{M_W^2}{4M_Z^2}\right)^{\frac{1}{2}} \tau_3, \\
g^2 &= \left[g^{(\mathrm{V})}\right]^2 + \left[g^{(\mathrm{A})}\right]^2 .
\end{aligned}
\tag{B.7}
$$

REFERENCES

1. UA2 Collaboration, CERN preprint CERN-EP/88-134 (1988).
2. R.K. Ellis, G. Martinelli and R. Petronzio, *Nucl. Phys.* **B211** (1983), 106.
3. A. Bawa and J. Stirling, *Phys. Lett.* **203B** (1988), 172.
4. S. Ellis, R. Kleiss and W. Stirling, *Phys. Lett.* **154B** (1985), 435; *Phys. Lett.* **163B** (1985) 261.
5. G. Altarelli, R.K. Ellis, M. Greco and G. Martinelli, *Nucl. Phys.* **B246** (1984), 12.
6. C. Davies and W. Stirling, *Nucl. Phys.* **B244** (1984), 337; C. Davies, B. Webber and W. Stirling, *Nucl. Phys.* **B256** (1985), 413.
7. G. Altarelli, *Phys. Rept.* **81** (1982), 1; A. Buras, *Rev. Mod. Phys.* **52** (1980), 199.
8. K. Kajantie and J. Lindfors, *Nucl. Phys.* **B146** (1978), 465.
9. M. Diemoz, F. Ferroni, E. Longo, and G. Martinelli, *Z. Phys.* **C39** (1988), 21.
10. G. Altarelli, R.K. Ellis and G. Martinelli, *Nucl. Phys.* **B157** (1979), 461.
11. M. Chanowitz, M. Furman and I. Hinchliffe, *Nucl. Phys.* **B159** (1979), 225.
12. J.C. Collins, private communication.
13. G. Bodwin, *Phys. Rev.* **D31** (1965), 2616; **D34** (1986) 3932; J. Collins, D. Soper and G. Sterman, *Nucl. Phys.* **B261** (1985), 104; **B308** (1988) 833.
14. G. 't Hooft and M. Veltman, *Nucl. Phys.* **B44** (1972), 189; P. Breitenlohmer and D. Maison, *Comm. Math. Phys.* **52** (1977), 11; and for a good introduction, see J.C. Collins, *Renormalization* (Cambridge University Press: Cambridge, 1984).

15. G. Altarelli, R.K. Ellis and G. Martinelli, *Nucl. Phys.* **B157** (1979), 461; J. Kubar-André, M. Le Bellac, J. Mennier and G. Plaut, *Nucl. Phys.* **B175** (1980), 251. See in particular eqs. (87) and (89) of Ref. [5].

16. UA1 Collaboration, *Phys. Lett. B* **193** (1987), 389; UA2 Collaboration, presented by P. Jenni in 1987 International Symposium on Lepton and Photon Interactions at High Energies, Hamburg, 1987.

17. G. Altarelli, R.K. Ellis, and G. Martinelli, *Z. Phys.* **27** (1985), 617.

FIGURE CAPTIONS

1) Leading diagrams for $q\bar{q} \to g\gamma^*$. The looped lines are gluons; the wavy, unlooped lines are photons or Ws.

2) Next-to-leading diagrams for $q\bar{q} \to g\gamma^*$.

3) Diagrams for $q\bar{q} \to gg\gamma^*$.

4) Diagrams for $q\bar{q} \to q\bar{q}\gamma^*$.

5) Diagrams for $qq \to qq\gamma^*$.

6) Diagram for $|\mathrm{G}_2|^2$.

7) The two routings of q_T for $2\mathrm{Re}(\mathrm{F}_6^*\mathrm{F}_8)$.

8) Application of the Ward identity.

9) The divergence of $2\mathrm{Re}(\mathrm{F}_5^*\mathrm{F}_8)$ that cancels the first one of Fig. 7.

10) W (solid) and Z (dashed) production at $\sqrt{s} = 1.8$ TeV. In each case, the theoretical error estimate is delineated by the two lines.

11) Predictions and experiment for W production at $\sqrt{s} = 630$ GeV. The two lines delineate the estimated error of the theoretical calculation.

12) $\mathrm{d}\sigma(M^2 = Q^2)/\mathrm{d}\sigma^{(1)}(M^2 = Q^2)$ and $\mathrm{d}\sigma(M^2 = q_T^2)/\mathrm{d}\sigma^{(1)}(M^2 = Q^2)$ where $\mathrm{d}\sigma$ means $\mathrm{d}\sigma/\mathrm{d}(q_T^2)$ and $\mathrm{d}\sigma^{(1)}$ is the first order contribution alone. Quantities are for W^+ production at $\sqrt{s} = 1.8$ TeV. The dashed line is $\mathrm{d}\sigma^{(1)}(M^2 = q_T^2)/\mathrm{d}\sigma^{(1)}(M^2 = Q^2)$.

13) The dependence of $\mathrm{d}\sigma/\mathrm{d}(q_T^2)$ on the factorization scale M. This is for W^+ production at $\sqrt{s} = 1.8$ TeV and q_T =100 GeV. Separate lines are given for Λ(4 flavors) = 160, 260, 360 MeV. Both 1st and 1st+2nd order results are shown.

14) Same as Figure 13 but $q_T = 20$ GeV.

15) Relative contributions of different processes to W production at $\sqrt{s} = 1.8$ TeV using $M^2 = Q^2$. First order contributions are (A) $q\bar{q} \to gW$ and (B)

$qg \to qW$. Second order contributions are from (C) $[q\bar{q} \to gW + ggW] + |\mathrm{F}_1 + \mathrm{F}_2|^2$, (D) $qg \to qW + qgW$ and $\bar{q}g \to \bar{q}W + \bar{q}gW$, (E) $gg \to q\bar{q}W$, (F) remaining $q\bar{q} \to q\bar{q}W$, and (G) $qq \to qqW$ and $\bar{q}\bar{q} \to \bar{q}\bar{q}W$.

16) Same as Fig. 15 but at $\sqrt{s} = 630$ GeV.

TABLE CAPTIONS

1: $(\mathrm{d}\sigma/\mathrm{d}q_T)/q_T/\sigma$ in Gev^{-2} as a function of q_T in GeV for $\sqrt{s} = 1.8$ TeV and $\Lambda(4\text{ flavors}) = 260$ MeV. Values for $M^2 = Q^2$ and $M^2 = q_T^2$ are given with the total cross-section σ evaluated at $M^2 = Q^2$ and $M^2 = \langle q_T^2 \rangle$ respectively.

2: Same as Table 1 but for $\sqrt{s} = 630$ GeV.

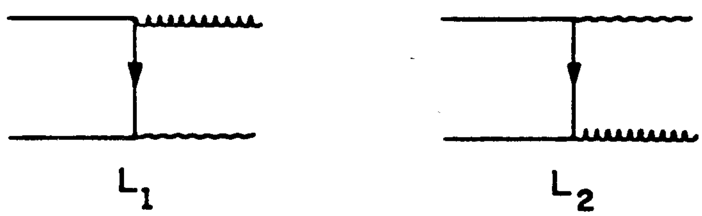

FIGURE 1

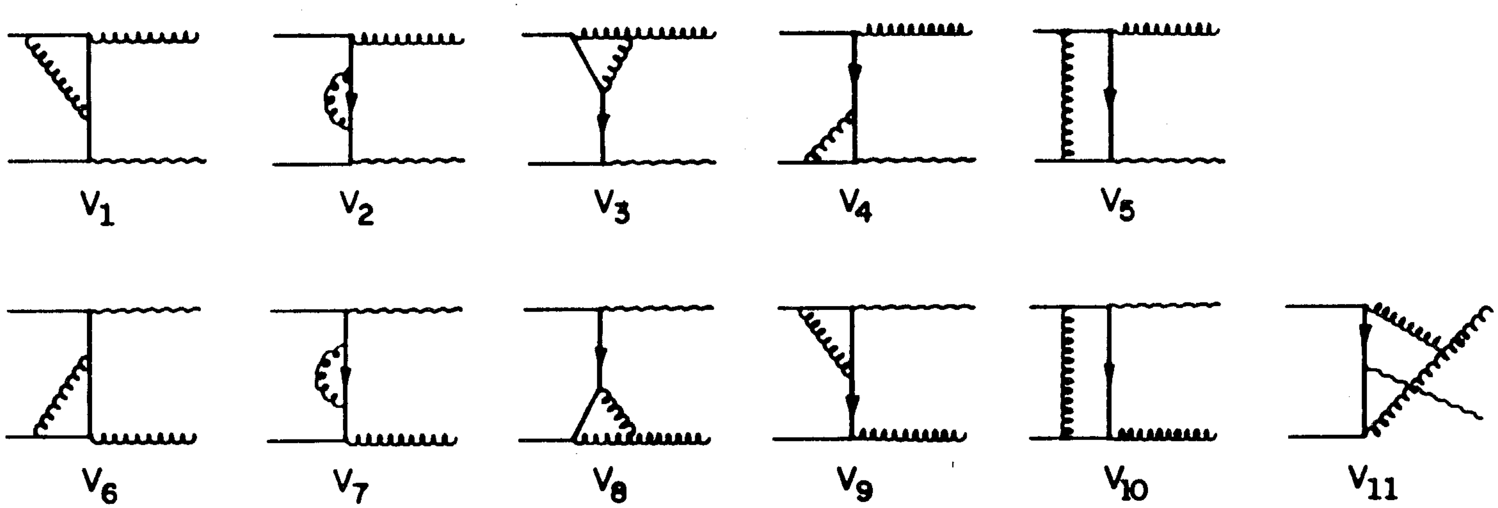

FIGURE 2

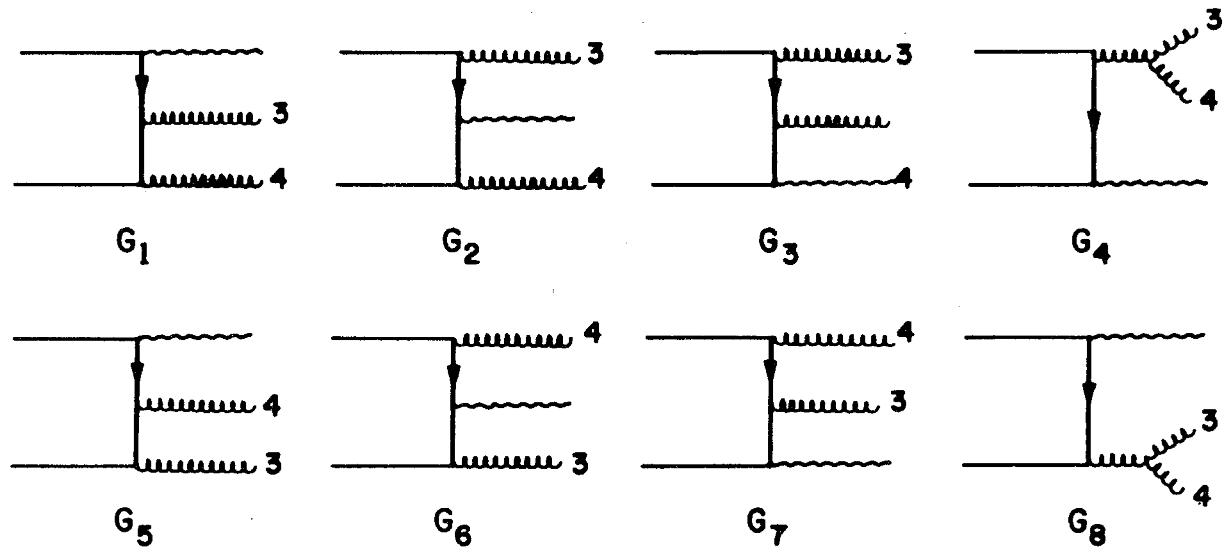

FIGURE 3

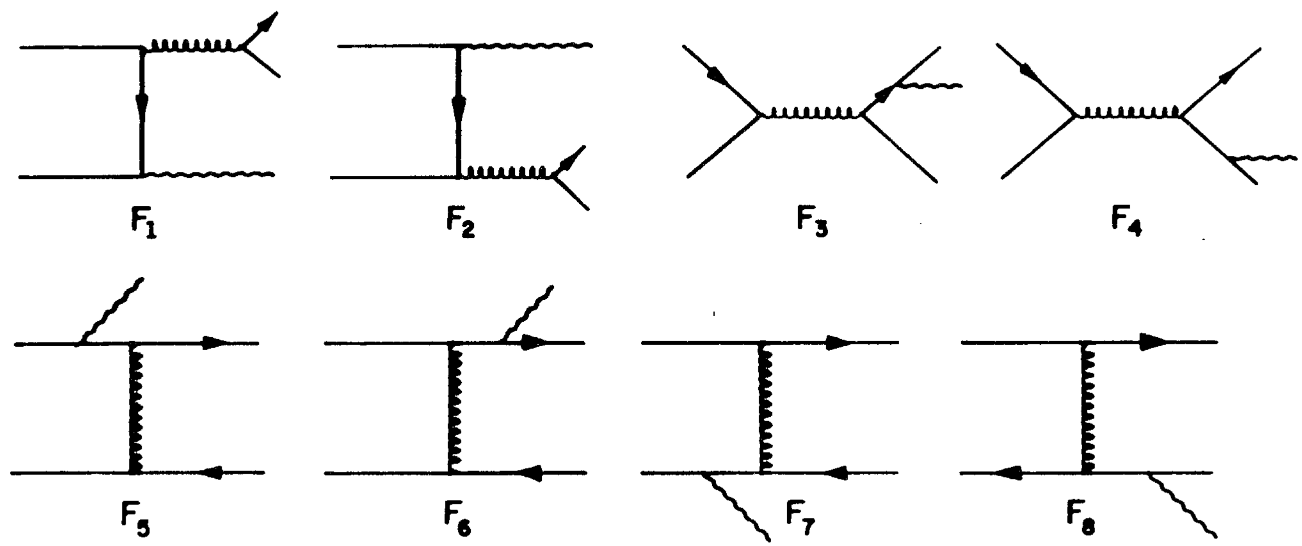

FIGURE 4

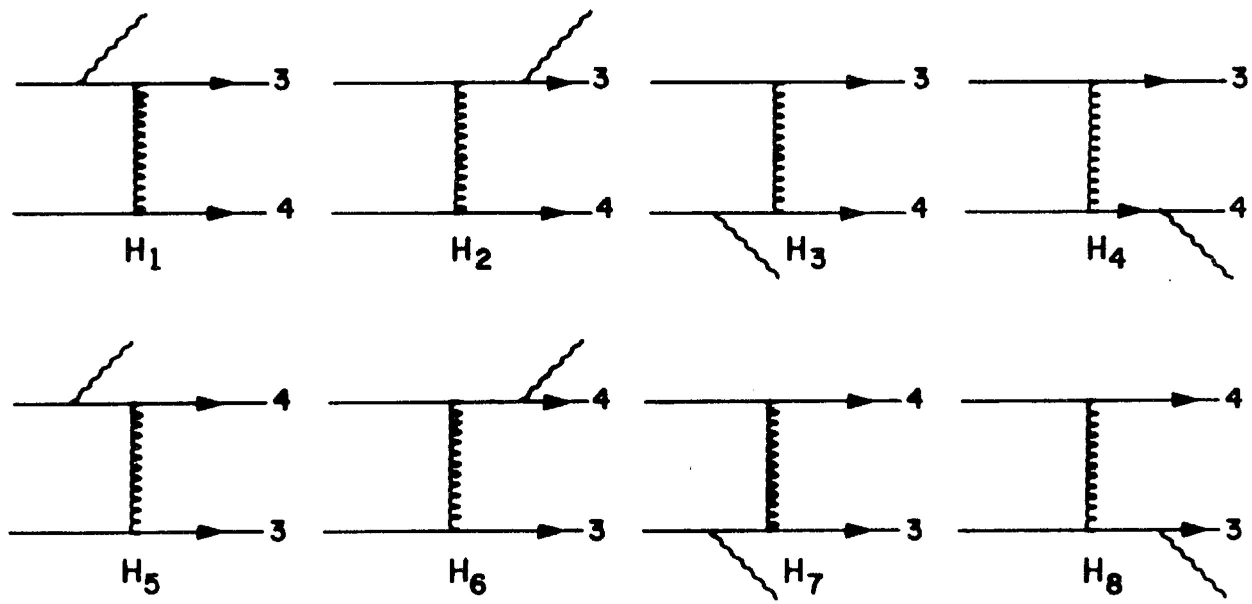

FIGURE 5

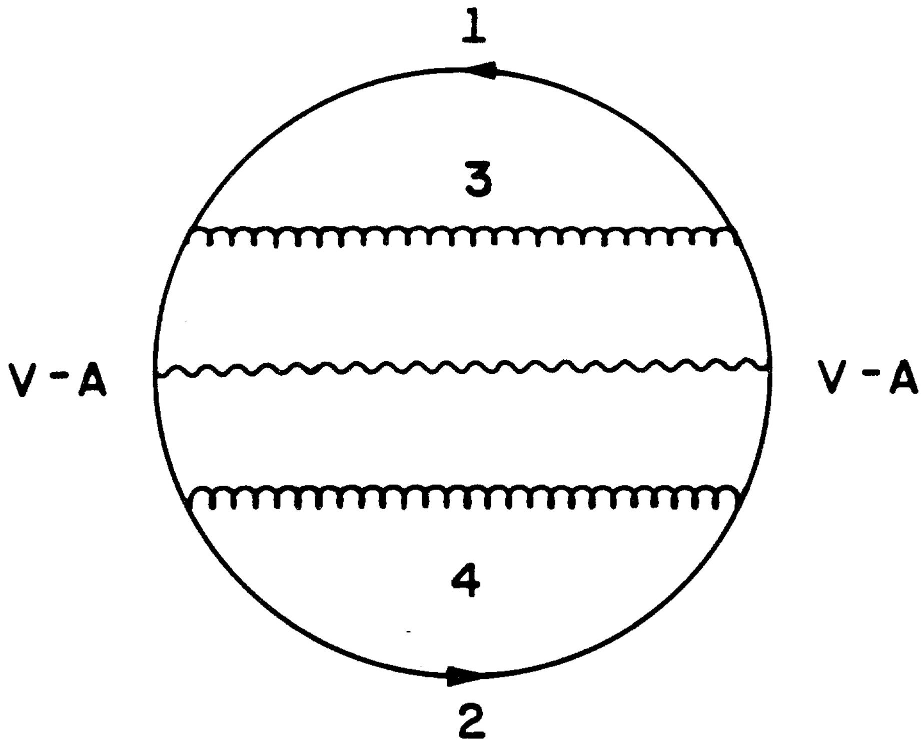

FIGURE 6

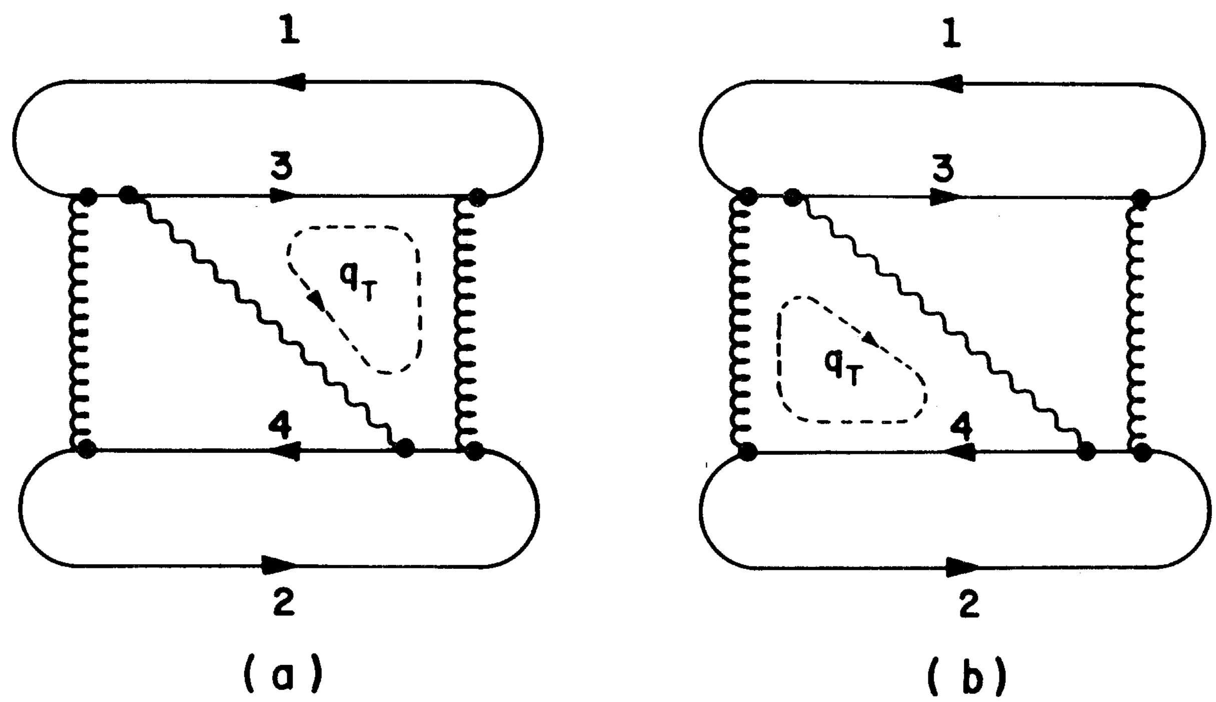

FIGURE 7

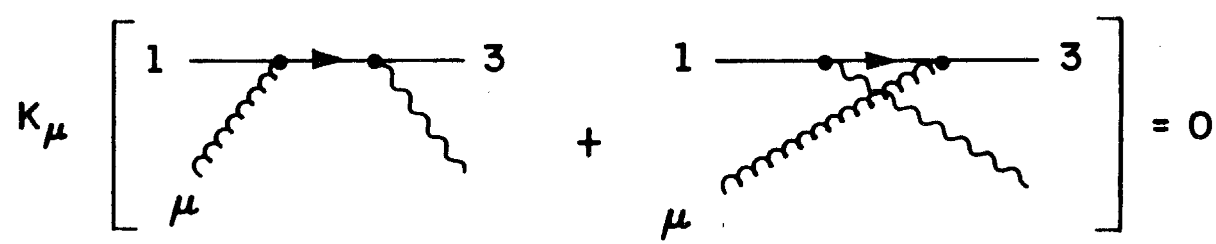

FIGURE 8

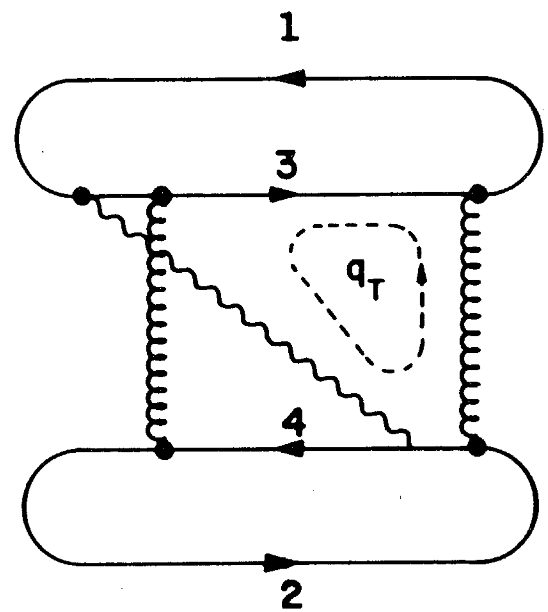

FIGURE 9

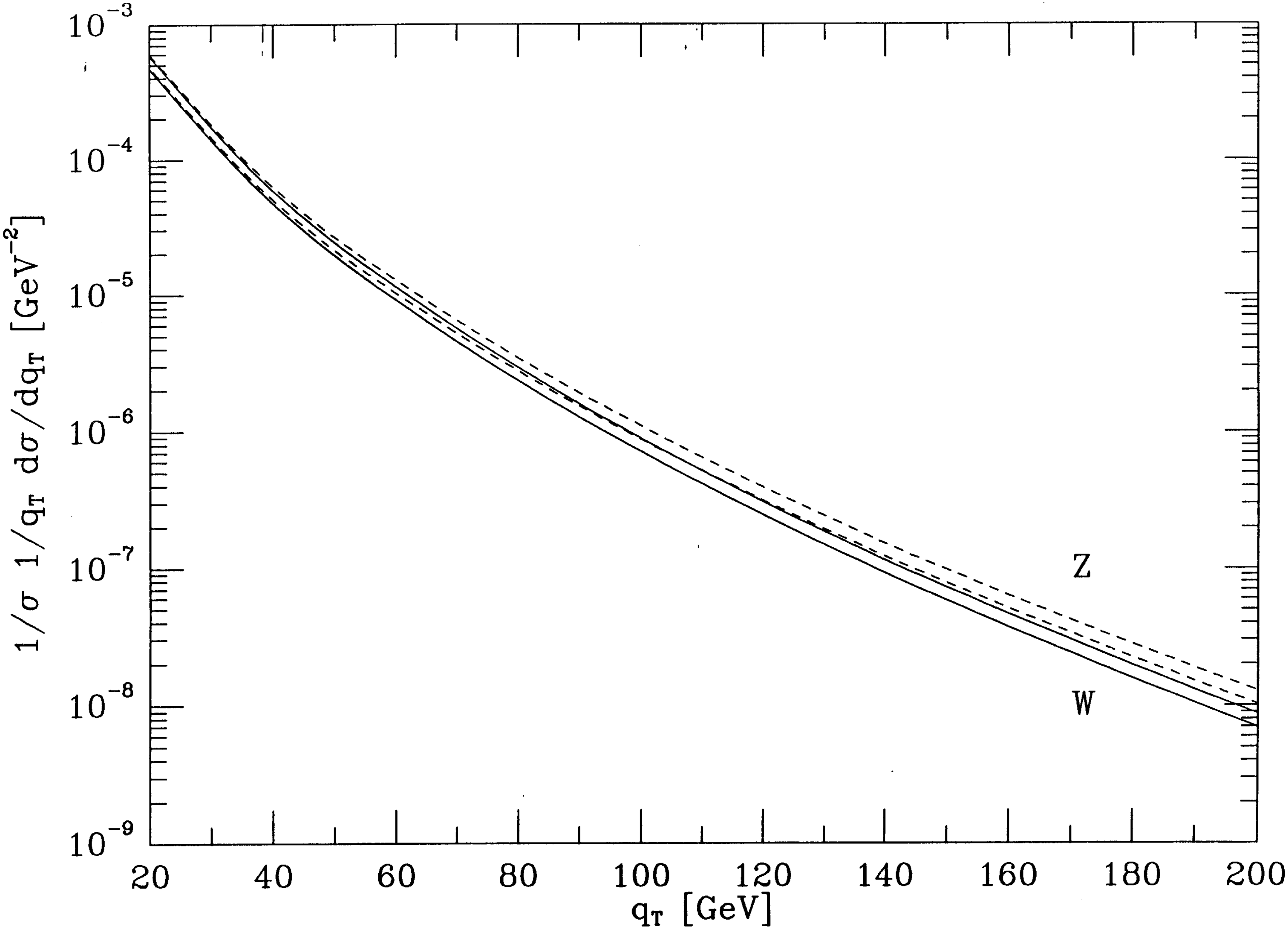

10^-3
10^-4
10^-5
10^-6
10^-7
10^-8
10^-9
1/σ 1/q_T dσ/dq_T [GeV^-2]
20
40
60
80
100
120
140
160
180
200
q_T [GeV]
Z
W

Figure 10.

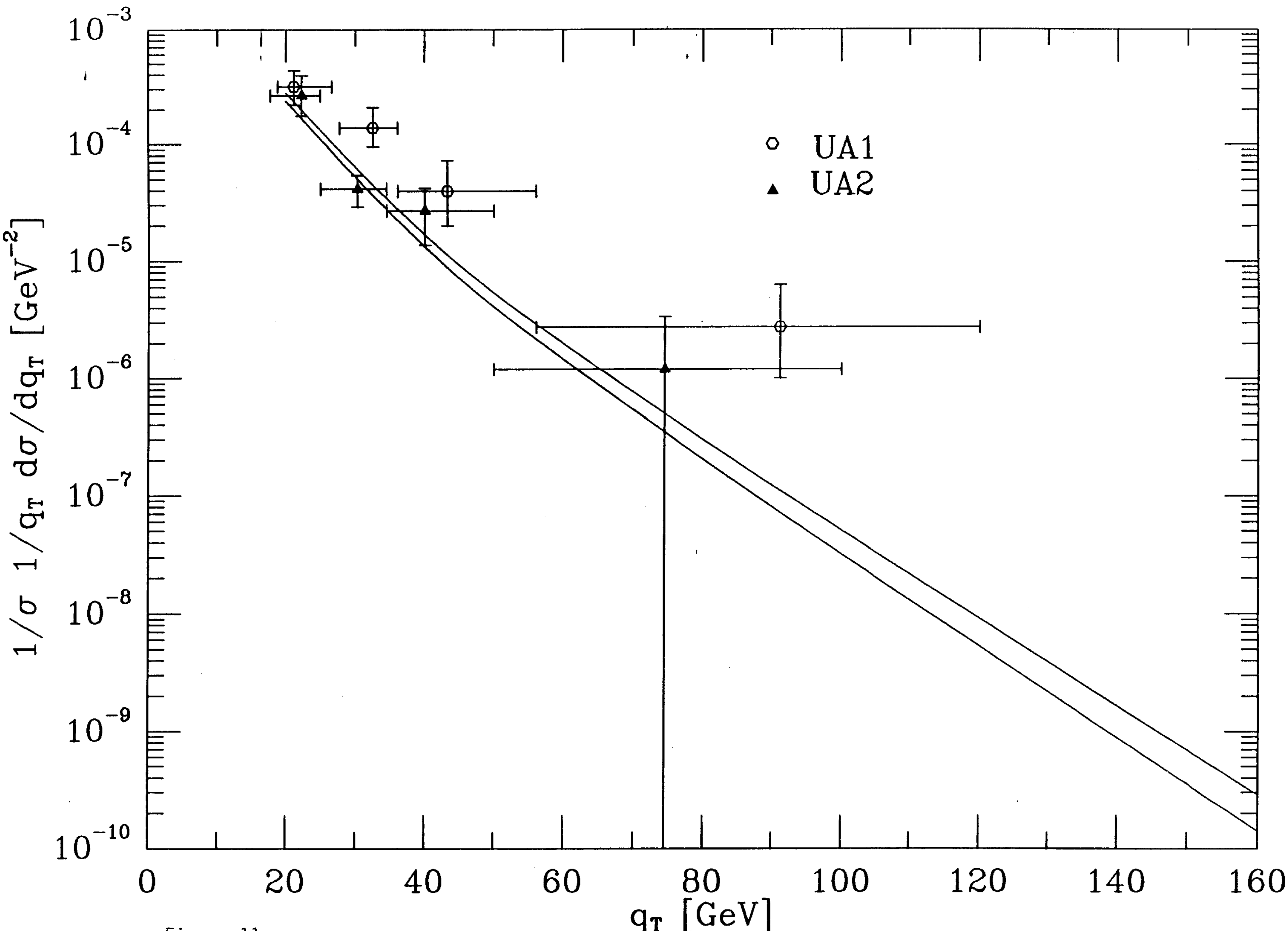
UA1
UA2
1/σ 1/q_T dσ/dq_T [GeV^-2]
q_T [GeV]
10^-3
10^-4
10^-5
10^-6
10^-7
10^-8
10^-9
10^-10
0
20
40
60
80
100
120
140
160

Figure 11.

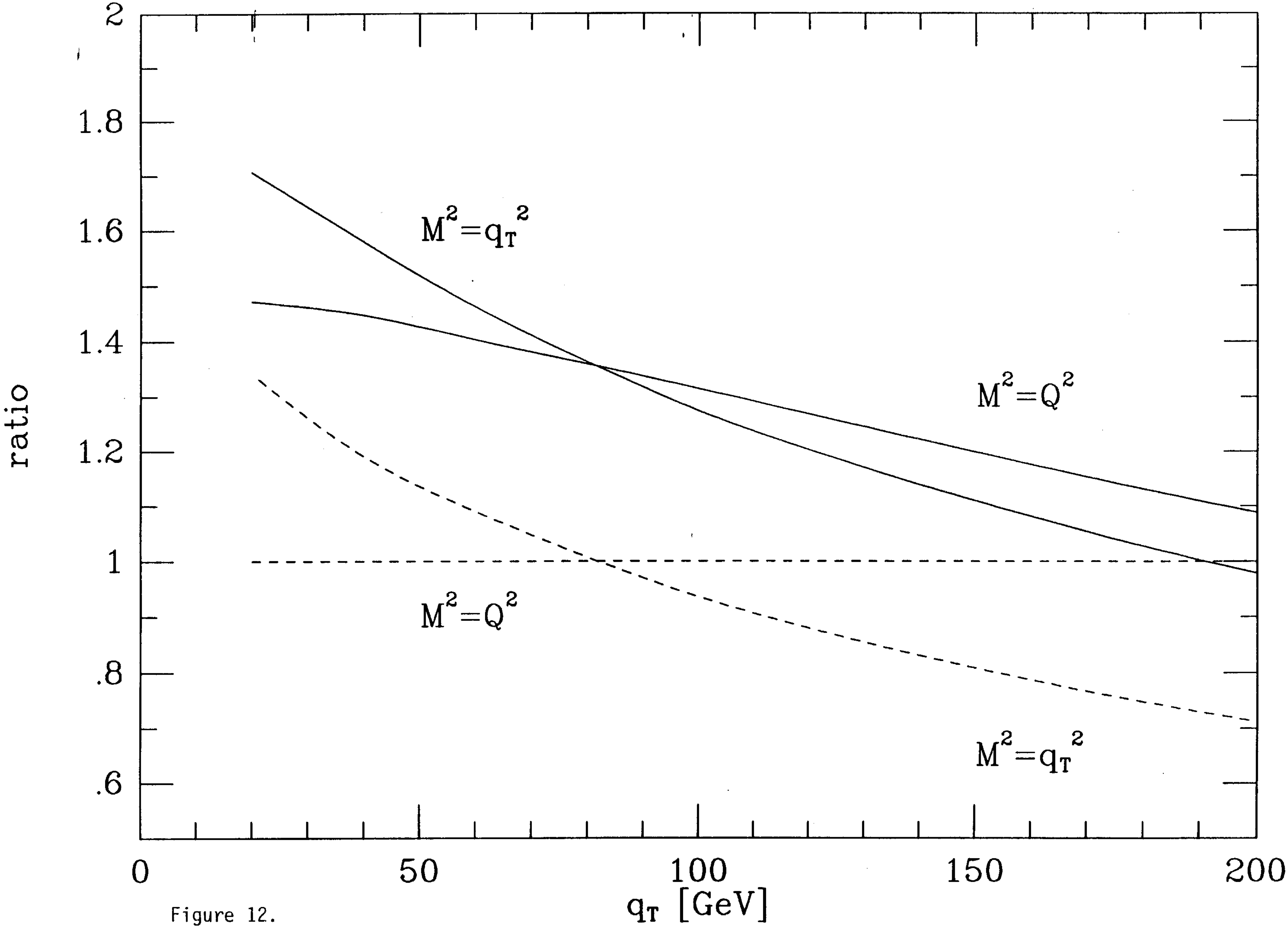

ratio
2
1.8
1.6
1.4
1.2
1
.8
.6
0
50
100
150
200
q_T [GeV]
$M^2=q_T^2$
$M^2=Q^2$
$M^2=Q^2$
$M^2=q_T^2$

Figure 12.

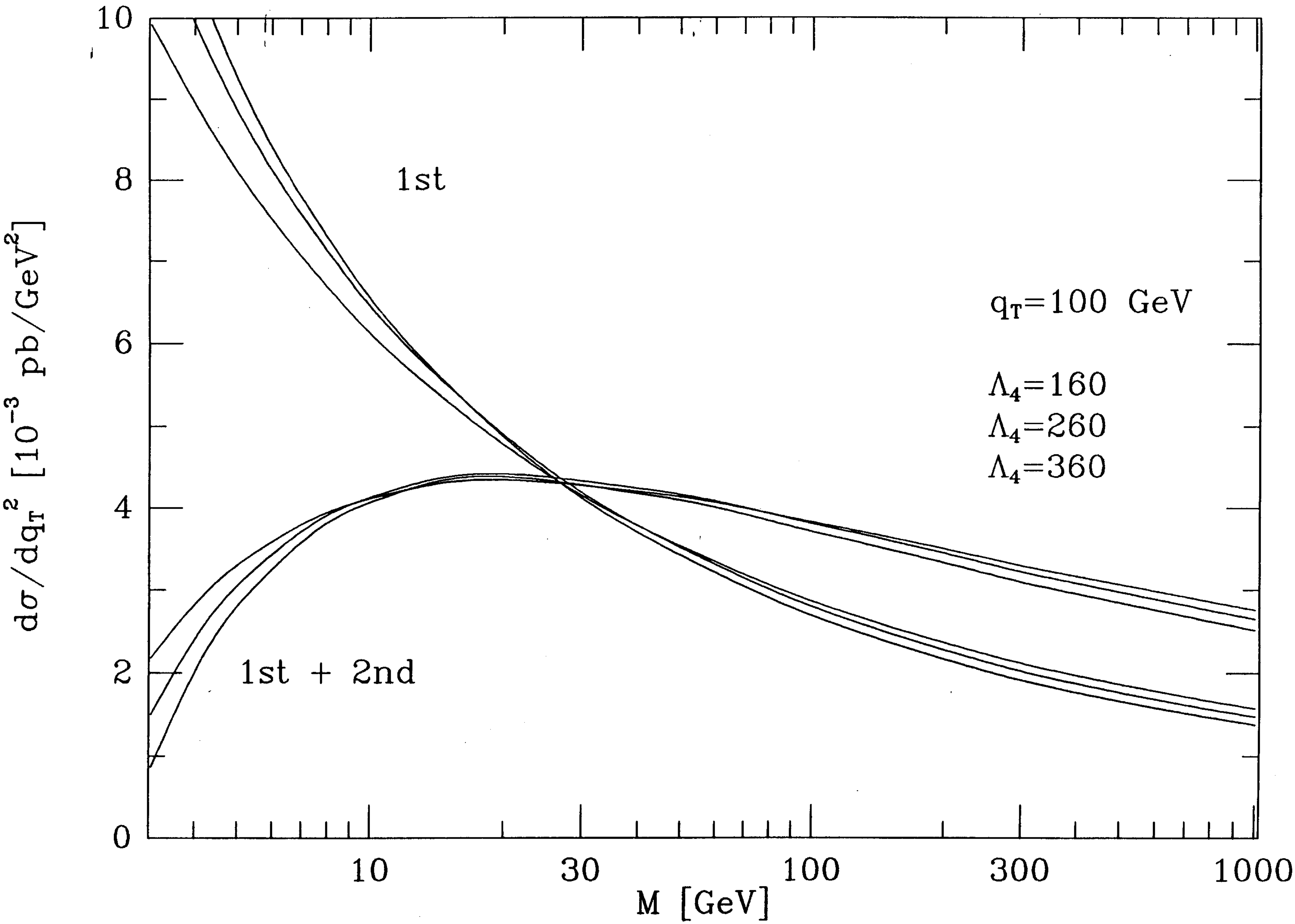
10
8
6
4
2
0
$d\sigma/dq_T^2$ [10^{-3} pb/GeV^2]
1st
1st + 2nd
q_T=100 GeV
Λ_4=160
Λ_4=260
Λ_4=360
10
30
100
300
1000
M [GeV]

Figure 13.

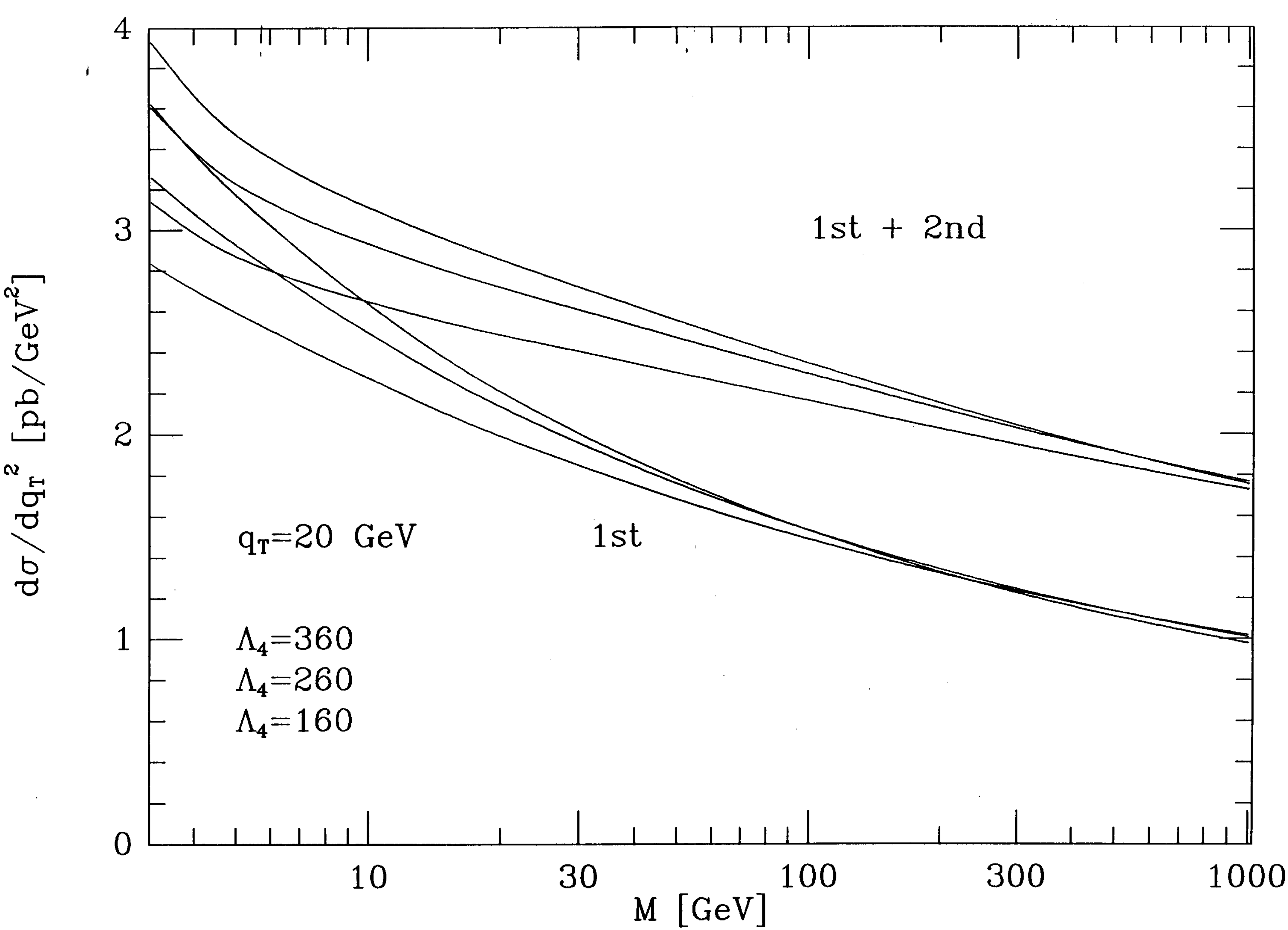

4
3
2
1
0
10
30
100
300
1000
M [GeV]
dσ/dq_T^2 [pb/GeV^2]
1st + 2nd
1st
q_T=20 GeV
Λ_4=360
Λ_4=260
Λ_4=160

Figure 14.

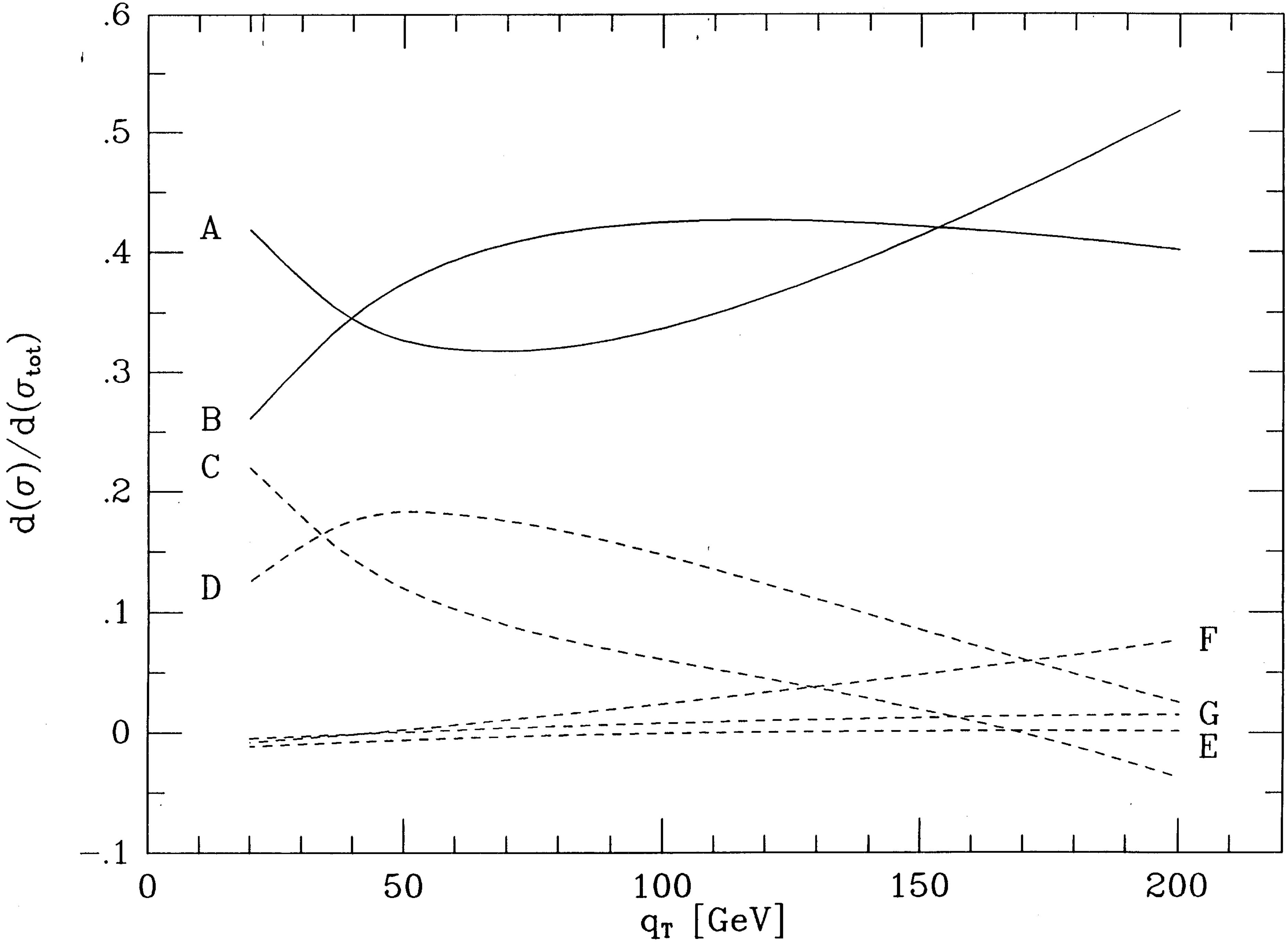

Figure 15.

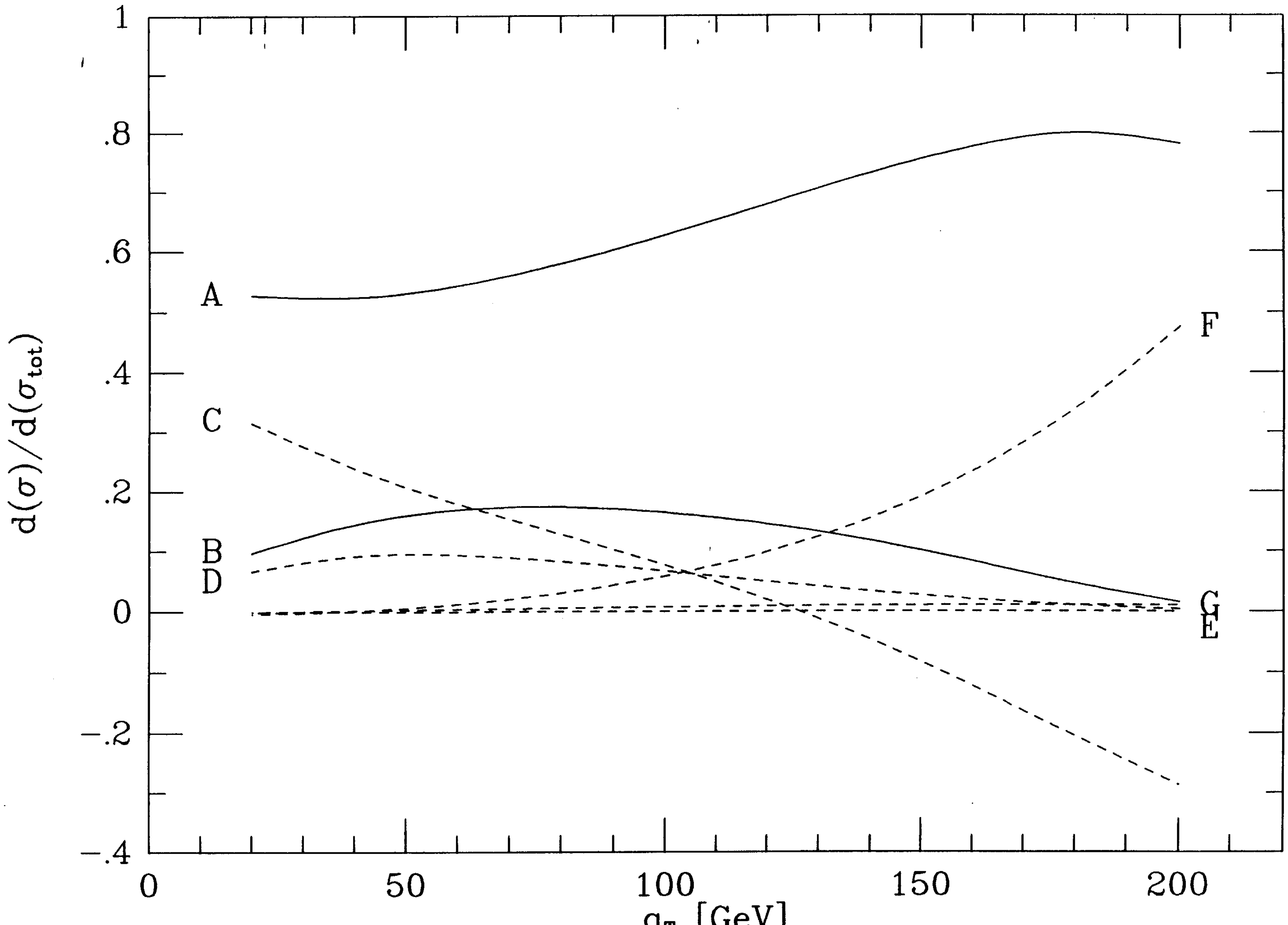

Figure 16.

q_T	W production		Z production	
	$M^2 = Q^2$	$M^2 = q_T^2$	$M^2 = Q^2$	$M^2 = q_T^2$
20	4.85×10^{-4}	5.70×10^{-4}	5.03×10^{-4}	5.80×10^{-4}
40	5.02×10^{-5}	5.56×10^{-5}	5.42×10^{-5}	5.91×10^{-5}
60	1.00×10^{-5}	1.06×10^{-5}	1.13×10^{-5}	1.18×10^{-5}
80	2.62×10^{-6}	2.67×10^{-6}	3.10×10^{-6}	3.12×10^{-6}
100	8.10×10^{-7}	7.98×10^{-7}	9.99×10^{-7}	9.75×10^{-7}
120	2.81×10^{-7}	2.70×10^{-7}	3.60×10^{-7}	3.44×10^{-7}
140	1.06×10^{-7}	1.00×10^{-7}	1.41×10^{-7}	1.33×10^{-7}
160	4.30×10^{-8}	4.01×10^{-8}	5.92×10^{-8}	5.49×10^{-8}
180	1.84×10^{-8}	1.69×10^{-8}	2.61×10^{-8}	2.40×10^{-8}
200	8.21×10^{-9}	7.49×10^{-9}	1.21×10^{-8}	1.10×10^{-8}

Table 1.

q_T	W production		Z production	
	$M^2 = Q^2$	$M^2 = q_T^2$	$M^2 = Q^2$	$M^2 = q_T^2$
20	2.65×10^{-4}	2.48×10^{-4}	2.88×10^{-4}	2.56×10^{-4}
40	1.64×10^{-5}	1.36×10^{-5}	1.93×10^{-5}	1.54×10^{-5}
60	1.93×10^{-6}	1.51×10^{-6}	2.46×10^{-6}	1.85×10^{-6}
80	2.91×10^{-7}	2.15×10^{-7}	4.02×10^{-7}	2.88×10^{-7}
100	4.88×10^{-8}	3.44×10^{-8}	7.39×10^{-8}	5.06×10^{-8}
120	8.61×10^{-9}	5.89×10^{-9}	1.43×10^{-8}	9.56×10^{-9}
140	1.53×10^{-9}	1.01×10^{-9}	2.77×10^{-9}	1.82×10^{-9}
160	2.62×10^{-10}	1.67×10^{-10}	5.20×10^{-10}	3.36×10^{-10}

Table 2.